

LANDSLIDE SUSCEPTIBILITY MAPPING OF THE  
GHURMI-DHAD KHOLA AREA IN EASTERN NEPAL  
USING GIS

A DISSERTATION  
(COURSE NO: GEO 639)

SUBEG MAN BIJUKCHHEN  
EXAM ROLL NO: 5542

SUBMITTED TO  
**CENTRAL DEPARTMENT OF GEOLOGY**  
INSTITUTE OF SCIENCE AND TECHNOLOGY  
TRIBHUVAN UNIVERSITY  
KIRTIPUR, KATHMANDU

IN PARTIAL FULFILMENT OF THE REQUIREMENTS FOR  
THE MASTER'S DEGREE OF SCIENCE IN GEOLOGY  
(ENGINEERING GEOLOGICAL TECHNIQUES)  
JUNE, 2011 (Ashad, 2068)



# TRIBHUVAN UNIVERSITY

CENTRAL DEPARTMENT OF GEOLOGY

OFFICE OF THE HEAD OF DEPARTMENT

Kirtipur, Kathmandu

Nepal

Ref No:

## Recommendation

Date: 17 June, 2011

It is certified that Mr. SUBEG MAN BIJUKCHHEN has worked satisfactorily for his Master's Degree dissertation under our guidance and supervision. He has worked enthusiastically with sincere interest. The dissertation entitled 'LANDSLIDE SUSCEPTIBILITY MAPPING OF THE GHURMI-DHAD KHOLA AREA IN EASTERN NEPAL USING GIS' embodies the candidate's own work. We, hereby, recommend the dissertation for approval.

.....  
Supervisor  
Prof. Dr. Megh Raj Dhital  
Head

.....  
Co-supervisor  
Mr. Prabin Kayastha  
Vrije Universiteit Brussel

Tel. No.: 4332449, 4333085  
E-mail: tugeology@wlink.com.np



# TRIBHUVAN UNIVERSITY

CENTRAL DEPARTMENT OF GEOLOGY

OFFICE OF THE HEAD OF DEPARTMENT

Kirtipur, Kathmandu

Nepal

Ref No:

## Letter of Apporval

Date: .....

The dissertation presented by Mr. SUBEG MAN BIJUKCHHEN entitled 'LANDSLIDE SUSCEPTIBILITY MAPPING OF THE GHURMI-DHAD KHOLA AREA IN EASTERN NEPAL USING GIS' has been accepted as the partial fulfilment of the requirements for the Master's Degree of Science in Geology.

.....  
Head  
Prof. Dr. Megh Raj Dhital

.....  
External Examiner

.....  
Supervisor  
Prof. Dr. Megh Raj Dhital

.....  
Co-supervisor  
Mr. Prabin Kayastha

## **ACKNOWLEDGEMENTS**

I would like to express my sincere gratitude to Prof. Dr. Megh Raj Dhital, Head of Central Department of Geology, Tribhuvan University for his invaluable guidance, consistent support and supervision throughout this work. I am indebted to him for his field supervision and suggestions in spite of his busy schedule.

I am much indebted to Dr. Kamala Kant Acharya, Assistant Lecturer, Tribhuvan University and Mr. Prabin Kayastha, Vrije Universiteit Brussel for guiding and providing valuable suggestions, help and support throughout the work. Without their kind help, support and guidance, this work would not have come in the present form. I am much obliged to Dr. Chandra Prakash Poudyal, Assistant Lecturer, Central Department of Geology for his worthy suggestions, help and support.

I am also thankful to the Nepal Academy of Science and Technology (NAST) for providing me a partial financial support as grant-in-aid for dissertation for excellent student in M.Sc.

I express sincere thanks to my senior Mr. Sudip Shrestha, Department of Survey for his kind co-operation and support during this work. I am equally thankful to my colleagues Babu Ram Gyawali, Chintan Timsina, Bishow Raj Silwal and Sobit Thapaliya for their continued support, invaluable suggestions and help throughout the work. I thank my friend Niraj Pradhananga, Department of Hydrology and Meteorology for providing necessary data for the work. I am equally obliged to all the members and friends of CDG, TU for their kind cooperation.

Lastly I owe my deep gratitude to my parents and my brother for their prolonged support, encouragement and inspiration in every step of my study.

Subeg Man Bijukchhen

17 June 2011



## **Abstract**

*The present study focuses on preparation of landslide susceptibility maps of the Ghurmi-Dhad Khola area, eastern Nepal using Geographic Information System (GIS).*

*The study area consists of 77 landslides covering an area of 2.069 km<sup>2</sup>. The parameters considered for the study are geology, distance from faults and folds, distance from drainage, rock and soil type, land cover, slope aspect, slope angle and altitude. The detailed geological map of the study area was prepared along with other thematic maps for the susceptibility analysis. The methods followed for the susceptibility analysis were the heuristic and bivariate methods.*

*In heuristic method, index-based approach was used to assess the landslide susceptibility. According to the map, an area of 24.77% falls under the high susceptibility zone whereas 18.92% of area falls under medium susceptibility and 56.31% in the low susceptibility zone.*

*In landslide susceptibility assessment carried out using the statistical-index approach of bivariate analysis method, 28.03% of area is considered high susceptible for landslides and 21.08% of area falls under medium susceptibility zone. An area of 50.89% lies in the safe zone i.e. the low susceptibility zone.*

*The two susceptibility maps were identical and success rate of both the maps were above 80%. Similarly there was 80.19% agreement between the two landslide susceptibility maps prepared by two different methods.*

**Keywords:** *Landslide, susceptibility, index-based, heuristic, statistical-index, bivariate, Nepal.*

# CONTENTS

LIST OF FIGURES	
LIST OF PLATES	
LIST OF TABLES	
ABSTRACT	
<b>CHAPTER ONE- INTRODUCTION</b>	<b>1</b>
<i>Location and Accessibility</i>	2
<i>Topography and Drainage</i>	2
<i>Climate</i>	2
<i>Aims and Objectives</i>	4
<i>Methodology</i>	5
Desk Study	5
Fieldwork	5
Data Processing and Interpretation	6
<b>CHAPTER TWO- MASS MOVEMENT AND THEIR CLASSIFICATIONS</b>	<b>7</b>
<i>Classification of Mass Movements</i>	7
Falls	8
Topples	8
Slides	8
Lateral Spreads	9
Flows	10
Complex Movements	11
<i>Mass Movements in the Study Area</i>	11
Rock Falls	11
Slides	11
<b>CHAPTER THREE- GEOLOGY OF THE STUDY AREA</b>	<b>17</b>
<i>Regional Geology</i>	17
<i>Previous Work in the Study Area</i>	18
<i>Stratigraphy of the Study Area</i>	20
Lesser Himalayan Sequence	21
Higher Himalayan Crystallines	28

3.4 Geological Structures	30
3.4.1 Major Structures	30
3.4.3 Mesoscopic and Minor Structures	32
<b>CHAPTER FOUR- GIS OVERLAYS FOR SUSCEPTIBILITY ANALYSIS</b>	<b>34</b>
4.1 Causative Factors of Landslides	34
4.1.1 Geological Factors	34
4.1.2 Morphological Factors	35
4.1.3 Anthropogenic Factors	35
4.2 GIS Overlays or Thematic Maps for the Present Study	35
4.2.1 Landslide Inventory Map	36
4.2.2 Geological Map	37
4.2.3 Distance from Fault or Fold-axis	39
4.2.4 Distance from Drainage	41
4.2.5 Rock and Soil Distribution	43
4.2.6 Land cover	45
4.2.7 Slope Aspect	47
4.2.8 Slope Angle	49
4.2.9 Altitude	51
4.2.9 Precipitation	53
<b>CHAPTER SIX- LANDSLIDE SUSCEPTIBILITY MAPPING APPLYING HEURISTIC AND BIVARIATE METHODS</b>	<b>55</b>
5.1 Landslide Susceptibility Analysis Methods	55
5.2 Previous Works on Landslide Susceptibility Mapping in Nepal	57
5.3 Landslide Susceptibility Analysis in the Study Area	57
5.3.1 Heuristic Method for Landslide Susceptibility Mapping	57
5.3.2 Bivariate Method for Landslide Susceptibility Mapping	65
5.4 Comparison of Landslide Susceptibility Maps	73
5.4.1 Comparison Based on Landslide Density	73
5.4.2 Comparison Based on Success Rate Curve	74
5.4.3 Comparison Based on Agreed Area	75
<b>CHAPTER SIX- CONCLUSIONS AND DISCUSSIONS</b>	<b>77</b>
6.1 Conclusions	77
6.2 Discussions	79
<b>REFERENCES</b>	<b>a</b>

## LIST OF TABLES

Table 2.1 Classification of landslides (Varnes, 1978)

Table 3.1 Stratigraphy of the Ghurmi–Dhad Khola area

Table 4.1 Areal percentage of distance from drainage classes and occurrence of landslides in each class

Table 4.2 Percentage coverage of rock-soil classes and occurrence of landslides in each class

Table 4.3 Percentage coverage of land cover classes and occurrence of landslides in each class

Table 4.4 Percentage coverage of altitude classes and occurrence of landslides in each class

Table 4.5 Percentage coverage of rainfall classes and occurrence of landslides in each class

Table 5.1 Characteristics of landslide susceptibility methods (Van Westen et. al. 1997)

Table 5.2 Weight and ratings assigned to parameters

Table 5.3 Distribution of landslide susceptibility zones and landslide occurrence

Table 5.4 Derivation of weight values of parameter classes by bivariate method

Table 5.5 Distribution of landslide susceptibility zones and landslide occurrence in them

Table 5.6 Comparison of landslide densities of landslide susceptibility zones

Table 5.7 Agreed area and percentage area of heuristic and bivariate method, and area and percentage area of observed landslides in agreed area

## **LIST OF FIGURES**

Figure 1.1 Drainage map of the study area

Figure 1.2 Average monthly rainfall in the study area (Manebhanjyang Rainfall Station, 1980-2009)

Figure 2.1 Landslide distribution map with location points of fieldwork

Figure 3.1 Generalised geological map of Nepal showing the present study area (modified after Amatya and Jnawali, 1994)

Figure 3.2 Geological map of the Ghurmi-Dhad Khola area, eastern Nepal

Figure 4.1 Simplified geological map of the study area

Figure 4.2 Percentage of geological units and landslides occurring in them

Figure 4.3 Distance from faults and folds

Figure 4.4 Area covered by distance from fault-fold classes and landslides occurring in them

Figure 4.5 Distance from drainage

Figure 4.6 Rock and soil distribution map

Figure 4.7 Land cover map of the study area

Figure 4.8 Slope aspect map of the study area

Figure 4.9 Area percentage of aspect class and percentage of landslide occurrence

Figure 4.10 Slope angle map of the study area

Figure 4.11 Altitude map of the study area

Figure 4.12 Average rainfall map

Figure 5.1 Distribution of ratings for slope angle classes

Figure 5.2 Distribution of ratings for distance from drainage classes

Figure 5.3 Distribution of ratings for rock or soil map

Figure 5.4 Landslide Susceptibility Index obtained with index-based method

Figure 5.5 Classification of LSI values based on natural break method

Figure 5.6 Landslide Susceptibility Zonation map using index-based method

Figure 5.7 Landslide Susceptibility Index obtained with statistical-index method

Figure 5.8 Classification of LSI values based on natural break method

Figure 5.9 Landslide Susceptibility Zonation map using statistical-index method

Figure 5.10 Success rate curves of LSZ maps of heuristic and bivariate analysis methods

## **LIST OF PLATES**

Plate 2.1 Panoramic view of Bhadare Khola rock fall

Plate 2.2 Landslide below the Ragapur village

Plate 2.3 Landslide on the right bank of Bhalu Khola

Plate 2.4 Landslide in mid reach of Binas Khola

Plate 2.5 Landslide southeast of Simlebesi

Plate 2.6 Landslide in upper reach of the Bhadare Khola

Plate 3.1 Folded rock of the Para Khola Formation

Plate 3.2 Graphitic slate of the Madhavpur Slates exposed at Ramdu Khola

Plate 3.3 Typical interbanding greenish-grey phyllite and greenish-grey dolomite  
at location OW 25

Plate 3.4 Granitic intrusion in the Higher Himalayan Crystallines at OW 18

Plate 3.5 Position of the MCT at the saddle of Hilepani

Plate 3.6 Mesoscopic fold observed in the Higher Himalayan Crystallines at OW  
22

Plate 3.7 Disrupted quartz veins in the graphitic slate of the Madhavpur  
Formation at OW 92

# CHAPTER ONE

## INTRODUCTION

Nepal, being a country with rugged and fragile mountain topography, is prone to a number of natural disasters like landslides, floods, earthquakes, draughts, avalanches and glacial lake outburst floods. Landslides in Nepal often occur during or after heavy monsoon rainfall resulting in the loss of life and damage to the natural and built environment. This situation is further aggravated by anthropogenic factors such as deforestation, haphazard migration and settlement, unsound agricultural practices and unplanned developmental works. According to Arnold et al., (2006), Nepal lies in moderate to high landslide hazard zone. In this respect, the present study was carried out to investigate the state of landslide hazard in the Midlands of Nepal. The study area lies in the Lesser Himalayan zone of east Nepal. It is delineated to the south by the Sunkoshi River, on the east by the Dudhkoshi River, on the west by the Malung Khola and by the Dhuseni Khola on the north with a total area of about 141 km<sup>2</sup>. For the purpose of preparing a landslide susceptibility map of the study area a geological map, rock and soil map, distance from drainage, distance from faults or folds, land cover map, altitude map, slope angle map and slope aspect map were prepared. Using these thematic maps the susceptibility analysis was carried out applying heuristic (index-based) and bivariate (statistical-index) methods. The final susceptibility map was categorised into low, medium and high susceptibility classes.

This dissertation is organised into six chapters. The first chapter includes a brief introduction; location, topography, drainage and climate of the study area; aims and objectives and methodology of the present study. The second chapter deals with mass movements and their classification. The third chapter describes the geology of the study area. Chapter Four describes the causative factors of landslides and the thematic maps used for the susceptibility analysis. Chapter Five is about landslide susceptibility mapping of the area using two methods (viz. heuristic and bivariate), their results and comparisons. The sixth chapter gives the conclusions and discussions.



## **Location and Accessibility**

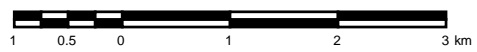
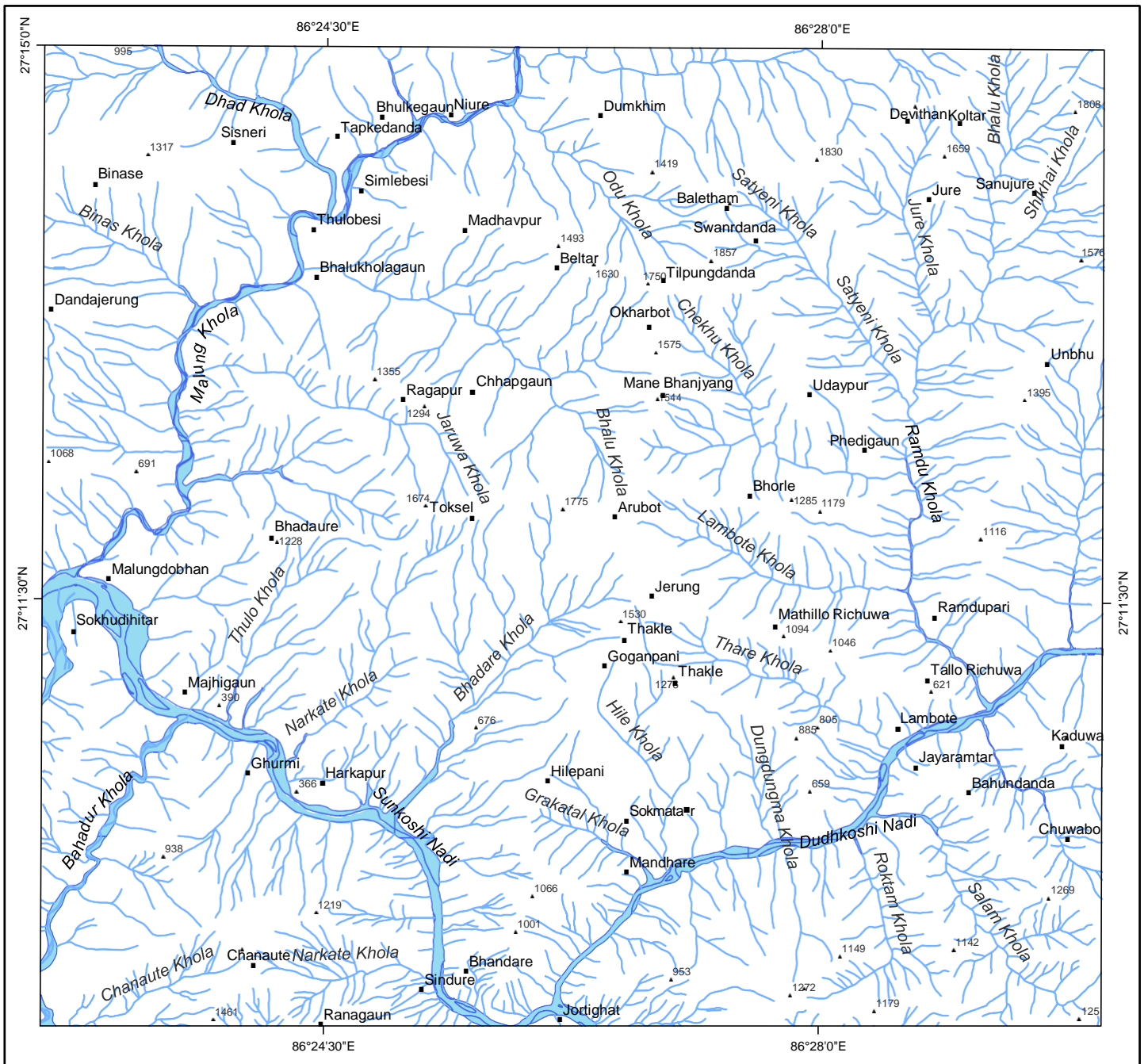
The study area lies in the Sagarmatha Zone, Eastern Nepal. It covers areas of Okhaldhunga District and small areas of Sindhuli, Udaypur and Khotang Districts as well, but the study mainly focuses on the Ghurmi-Dhad Khola area of the Okhaldhunga District. It covers the topographical map number 2786-14B (Department of Survey, Government of Nepal) of 1:25000 scale. It lies between latitudes 27°08'45" N to 27°15'00" N and longitudes 86°22'30" E to 86°30'00" E. (Figure 1.1) The area is facilitated by gravelled and earthen roads, tracks and foot trails. An all-weather motorable road connects it with Katari of the Udaypur District. Another motorable road connecting it with Khurkot of the Sindhuli District is under construction. The link roads joining the district headquarters of Okhaldhunga, Khotang and Solukhumbu pass through the study area.

## **Topography and Drainage**

The study area constitutes a hilly terrain exhibiting rugged topography with a diversity of landforms. The altitude ranges from 320 m at Jortighat to 1859 m at Baletham. It is drained by many rivers and streams, the Sunkoshi and the Dudhkoshi Rivers being the prominent. Both of these are snow-fed perennial rivers and the former flows into the area from northwest and the latter from the northeast. Other important rivers in the area are the Malung Khola, Dhad Khola, Bahadur Khola, Bhadare Khola, Ramdu Khola, Sodhu Khola, Dothe Khola and Dhuseni Khola, the tributaries of the main two rivers. Besides, there are numerous small rivers and streams feeding these rivers. The drainage pattern of the study area is essentially dendritic (Figure 1.1).

## **Climate**

The climate of any area is governed by altitude and physiographic characteristics. The study area experiences subtropical to temperate climate. As the altitude of the area varies from 300 m to 1900 m, the variability in climate is not uncommon. The temperature ranges from 5 to 35 °C with hot summer and warm winter in the river basins and warm summer and cold winter in higher altitudes.



- 1586  
▲ Spot Height
- Hilepani  
■ Village
- River

**LOCATION DIAGRAM**

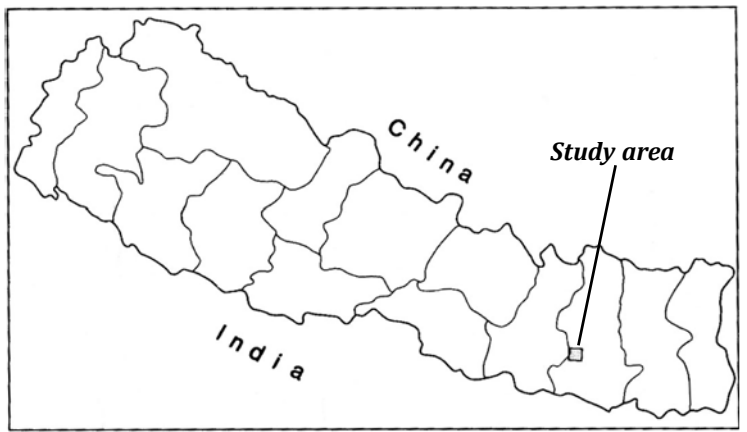


**Figure 1.1 Drainage map of the study area**

The period in which the area receives rainfall is not different from rest of the country with about 80% of all precipitation occurring in the monsoon starting from June to the end of September (Figure 1.2). The average annual precipitation of the area is 1080 mm. Rain intensities vary throughout the area with a maximum intensity of rainfall occurring on the south-facing slopes.

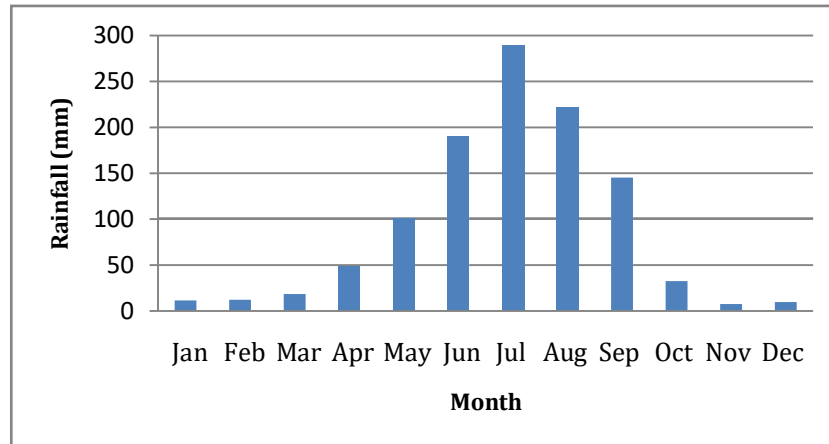


*Figure 1.2 Average monthly rainfall in the study area (Manebhanjyang Rainfall Station, 1980-2009)*

## **Aims and Objectives**

The purpose of present investigation was to collect geological and landslide data in order to prepare a geological map and landslide susceptibility maps of the study area with academic intents. The product of the study can be useful in planning, designing and implementing the developmental projects in the study area.

The aims of the present study can be summarised as:

- To prepare a detailed geological map of the study area with appropriate cross-sections
- To prepare landslide susceptibility maps based on heuristic and bivariate analysis methods using GIS and compare the resulting maps.

The reasons for selecting the area for the study were as follows.

- There has not been enough work with a purpose of making detailed geological map of the present area.
- The study area has many active landslides and parts of it are prone to sliding.
- The link roads joining the district headquarters of Okhaldhunga, Khotang and Solukhumbu pass through the study area and it is important to delineate the landslide susceptible areas for further development of the roads.

## **Methodology**

For the achievement of the above-mentioned aims, the study was conducted in four stages, viz. desk study, fieldwork, data processing and interpretation.

### **Desk Study**

Various maps, reports and data, journals and other publications related to the present study were collected and studied in detail. The topographic map of 2786-14B, 2786-10D (published by the Survey Department, Government of Nepal) and Google Earth® images were used for the study. The desk study provided some insight into and concept of the topographic, geological and landslide conditions of the study area.

### **Fieldwork**

Desk study was followed by a series of detailed fieldwork in the area. Different types of map required for the study were prepared based on the field study. Field data were collected to prepare the geological map of the study area. Similarly the data were used to prepare the landslide inventory map and the rock and soil map of the area.

Brunton Compass, topographic maps, geological hammer, GPS, magnifying glass, measuring tape, 10% hydrochloric acid and graph papers were used for the field study. The traverses were made along the Sunkoshi River, Dudhkoshi River, Sodhu Khola, Ramdu Khola, Malung Khola and Dhad Khola and the Harkapur–Okhaldhunga and Harkapur–Jayaramtar road sections and a number of other

streams, gulleys and foot trails. Attitude of beds or foliations was measured and plotted on the topographical map and contacts between different lithotypes were carefully delineated on the map. Geological structures like folds and faults were also depicted on the map.

The landslides not shown on the topographic maps were marked on the map to prepare the up-to-date landslide inventory map. Similarly a rock and soil map of the area was also prepared during the fieldwork.

### **Data Processing and Interpretation**

The data collected during the desk study and fieldwork were analysed and processed to give the final output. The data were used to develop a database for GIS analysis. Interpretation and presentation of the data were facilitated by the help of various types of computer software. The geological map and the cross-section were prepared using a variety of computer programmes.

For the analysis of landslide susceptibility, the collected data were used for preparation of various factor maps of the area, which were digitized. With the help of ArcGIS® and IDRISI Andes®, the analysis was performed using a series of digital maps with pixel resolution of 10 m. The analysis was performed by heuristic and bivariate methods. Both the susceptibility maps produced by two methods were later compared for their consistency.

In heuristic method index-based approach was used, where various causative factors of landslides were given weight or rank by an expert according to their relative importance in triggering the instability. The weights assigned to each parameter subclass were then combined to produce a landslide susceptibility map.

In bivariate analysis the area occupied by the instability within an attribute class is compared with the total area of that attribute class and then normalised by the ratio of the total landslide area and the watershed area. In the present study, the statistical-index method of bivariate analysis was applied to prepare a landslide susceptibility map.

## CHAPTER TWO

### MASS MOVEMENTS AND THEIR CLASSIFICATION

The mass movement is a phenomenon of denudation process, whereby soil or rock is displaced along the slope by mainly gravitational forces, usually occurring on unstable slopes due to various reasons (Safaei et al., 2010). Terzaghi (1950) defined the mass movement as a rapid displacement of a mass of rock, residual soil or sediment of the adjoining slope in which the centre of gravity of the moving mass advances in a downward and outward direction. Similarly, Varnes (1958) described it as the downward and outward movement of slope-forming materials, such as rocks, soils or artificial fills.

#### Classification of Mass Movements

Mass movements can be classified in many ways developed by different authors based on various criteria. But the most widely used classification system is that given by Varnes (1978). He classified them into five classes (fall, topple, slide, spread and flow) and a complex class combining two or more of the five classes. The classification system of Varnes (1978) is based on material type and the type of movement (Table 2.1).

*Table 2.1 Classification of landslides (Varnes, 1978)*

Type of movement		Type of material		
		Bedrock	Soil	
			Coarse	Fine
Falls		Rock fall	Debris fall	Earth fall
Topples		Rock topple	Debris topple	Earth topple
Slides	Rotational	Rock slump	Debris slump	Earth slump
	Translational	Rock block slide; rock slide	Debris block slide; Debris slide	Earth block slide; Earth slide
Lateral spreads		Rock spread	Debris spread	Earth spread
Flows		Rock flow (deep creep)	Debris flow (soil creep)	Earth flow (soil creep)
Complex slope movements (e.g., combination of two or more types)				

Different types of landslides are described below.

### **Falls**

A fall starts with the detachment of soil or rock from a steep slope along a surface on which little or no shear displacement takes place. The material then descends mainly through the air by falling, bouncing, or rolling (Varnes, 1996). According to Hutchinson (1988) secondary falls involve rock bodies already physically detached from cliff and merely lodged upon it. A fall generally occurs on slope of 45° to 90° and is a quick process.

Rock falls occur when pieces of rock on a steep slope are dislodged by weathering, erosion, excavation, etc., and they face down the slope. The rocks falling from the slope are in the form of blocks, but sometimes, these are broken into many small pieces as they collapse with others on the lower slope. Rock-fall is very common in steep mountainous terrain, where rock-fall debris accumulates at the base of steep slopes.

Debris falls involve a mixture of rock, soil, vegetation and regolith. A rock fall may dislodge other materials and cause the debris falls, especially on steep cliffs. Talus is the term used for the accumulated fallen mass at the base of the slope.

When the falling material has 80% or more of particles smaller than 2 mm, the upper limit of sand-sized particles (Varnes, 1978) it is known as earth falls.

### **Topples**

A topple is the forward rotation out of the slope of mass of soil or rock about a point or axis below the centre of gravity of the displaced mass. Toppling is sometimes driven by gravity exerted by material upslope of the displaced mass and sometimes by water or ice in cracks in the mass (Varnes, 1996).

### **Slides**

A slide is a down-slope movement of soil or rock mass occurring predominantly on the surface of rupture or on relatively thin zones of intense shear strain (Varnes, 1996). The slide can be rock-slides or debris-slides when rocks or

debris slide down a pre-existing surface, such as a bedding or joint or foliation surface. Piles of talus are common at the base of a rock slide or debris slide.

Rotational slides move along a surface of rupture that is curved and concave (Varnes, 1996). The movement results from forces that cause a turning moment about a point above the centre of gravity of the unit.

Translational slides occur when the mass displaces along a planar or undulating surface of rupture, sliding out over the original ground surface (Varnes, 1996). Such slides occur without any significant change in geometry of the unstable region (Lee et al., 1983). Generally the movement is structurally controlled by discontinuities and variations in shear strength between layers of bedded deposits, or by the contact between firm bedrock and overlying detritus. Block slides are translational slides in which the moving mass consists of a single unit of rock block that moves down slope (Deoja et al., 1991).

A slump is a type of failure involving rotational movement of rock or regolith that is downward and outward along a curved, concave-up surface. The upper surface of each slump block remains relatively undisturbed, as do the individual blocks.

### **Lateral Spreads**

A spread is defined as an extension of a cohesive soil or rock mass combined with a general subsidence of the fractured mass of cohesive material into softer underlying material (Varnes, 1996). The dominant mode of movement is lateral accommodated by shear or tensile fractures (Varnes, 1978). Lateral spreads involve the horizontal displacement of the surface. They often occur on gentle slopes. They are more common in fine grained soils, such as clay, especially if the soil has been remodelled or disturbed by construction, grading or similar activities. The failure in this case is caused by liquefaction, where increase in pore-water pressure of the saturated, loose, cohesionless sediments nearly reduces the effective stress of the soil mass to zero (Johnson and DeGraff, 1988) eventually liquefying the sediments.



## **Flows**

Flows may be considered to be progressive mass movements of soil of very low shear strength (Lee et al., 1983). The lower boundary of displaced mass may be a surface along which an appreciable differential movement has taken place or a thick zone of distributed shear (Cruden and Varnes, 1996).

Rock flows in bedrock include deformations that are distributed among many large or small fractures, or even micro fractures, without concentration of displacement along a through-going fracture (Varnes, 1978).

A debris flow is a very rapid to extremely rapid flow of saturated non-plastic debris in a steep channel (Hungr et al., 2001). It normally occurs when a landslide moves down-slope as a semi-fluid mass scouring, or partially scouring soils from the slope along its path initiated by heavy precipitation.

Debris avalanches are a type of very rapid to extremely rapid debris flow of large volume mixtures of rock and regolith that result from complete collapse of a mountainous slope.

An earth flow is a rapid or slower, intermittent flow-like movement of plastic, clayey earth (Hungr et al., 2001). It has a characteristic bowl-like depression at the head where the slope material becomes liquefied and flows out. It usually remains active for long periods, and generally tends to be narrow tongue-like features that begin at a scarp or small cliff. Even after its initial motion ceases it may be highly susceptible to renewed movement.

Mud flows are very rapid to extremely rapid flows of saturated plastic debris in a channel, involving significantly greater water content relative to the source material (Hungr et al., 2001). They occur on material containing about 50% of sand, silt and clay-sized particles that are well saturated and flow rapidly.

A creep is the imperceptibly slow, steady, downward movement of slope-forming soil or rock. Terzaghi (1950) described the creep as 'downhill movements which occur at an imperceptible rate.' The movement is essentially viscous enough to produce permanent deformation but too small to produce failures as in

landslides. A creep is indicated by curved tree trunks, bent fences or retaining walls, tilted poles and small soil ripples or ridges.

### **Complex Movements**

Slope movements involving two or more principal types of movements are called complex movements. For example, rolling rock blocks from higher elevations due to rock falls may cause debris slides at lower elevations.

### **Mass Movements in the Study Area**

There are various mass movements present in the study area, which were observed and delineated during the study (Figure 2.1). The mass movements are distributed in clusters in Bhadare Khola, Binas Khola and Bhalu Khola. The mass movements in the area vary from rock falls to rock and soil slides. As the main focus or emphasis of the present study was the identification and demarcation of the landslides, there was less effort on detailed analysis of the type and causes of the landslides. Hence complete information needed to classify and analyse causes of occurrence are lacking. Nevertheless an attempt is made here to describe a few of major mass movements of the area. Plates 2.1 to 2.6 depict some typical landslides observed in the area.

### **Rock Falls**

A large rock fall (Plate 2.1) is located in the mid reaches of the Bhadare Khola (OW 6 and OW 7, Figure 2.1). Its total affected area is more than 600 m x 500 m and the fall occurs in steep (more than 40°) rock slopes. The main cause of the failure may be the weak and fragile lithology. The rock fall is a major threat to the Harkapur–Hilepani section of the Katari–Okhaldhunga road.

### **Slides**

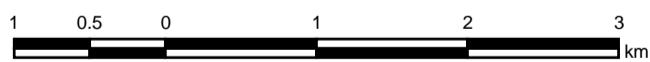
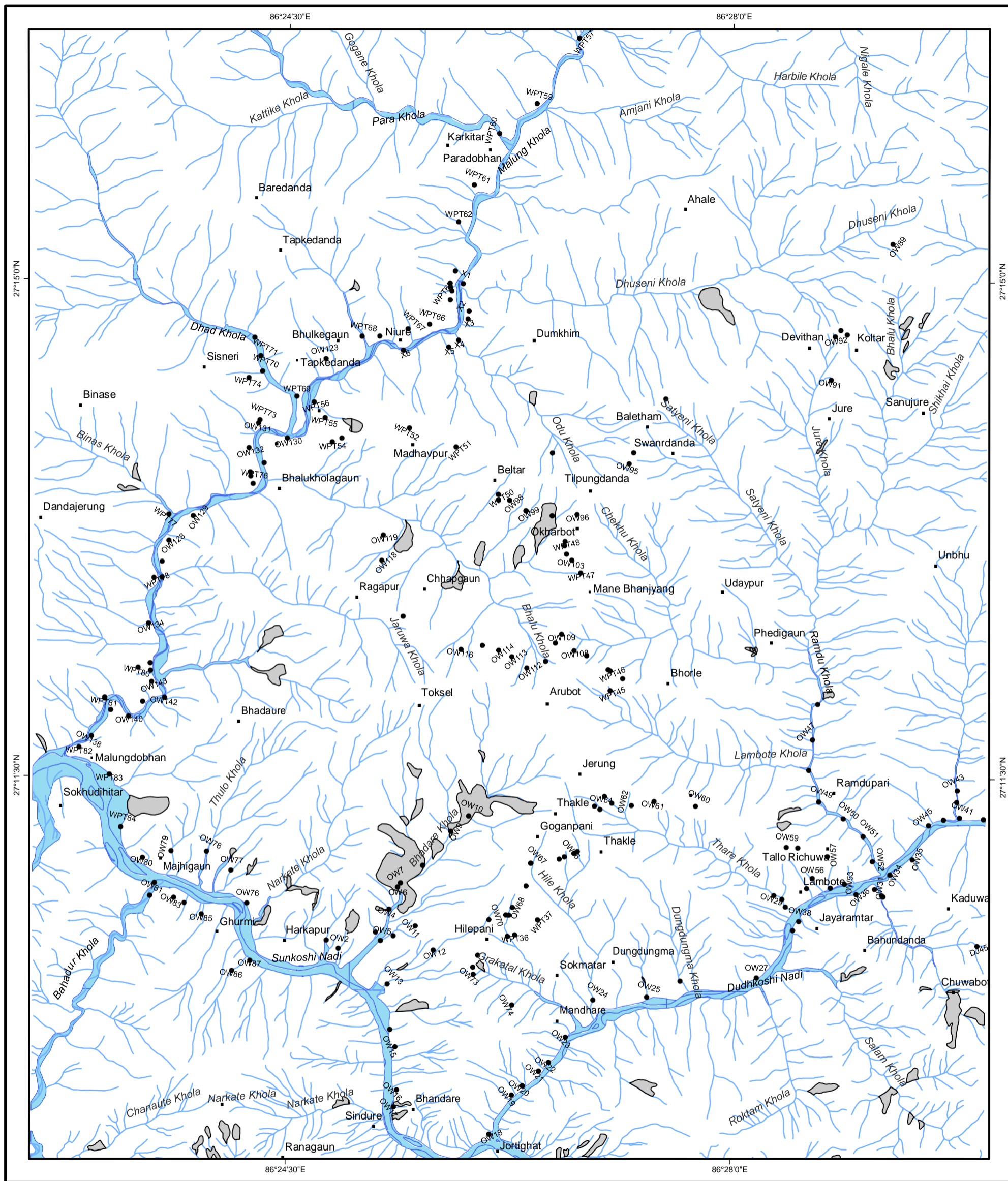
A translational earth slide (Plate 2.2) was observed on the left bank of the Bhalu Khola below the Ragapur village (east of OW 119). The slide is about 200 m x 300 m in dimension and is in active state. Extreme rainfall and gully erosion

coupled with steep slope of 35–45° may be the cause of the sliding. The agricultural lands of the Ragapur village are vulnerable to the slide.

A rock slide can be observed west of Okharbot, on the road from Manebhanjyang to Madhavpur (OW 100). The unplanned road cutting has aggravated the slide and it is a threat to the newly dug road. The slide is about 200 m wide and 500 m long, and is still actively moving.

A debris slide (Plate 2.5) was observed (east of WPT 55) southeast of Simlebesi. About 100 m x 250 m in dimension this landslide may have been triggered by fragile lithotype. Though the slide lies on the forest area, its talus deposit may be a threat to the agricultural land in the river basin.

Most of the mass movements are shallow, although some deep-seated movements are also found in the study area. A majority of mass movements are transitional slides and rock falls, with rock falls generally occurring on the southern slopes. The failures are concentrated in the southern study area near the Main Central Thrust. The lengths of a majority of mass movements are longer than their breadth and their size varies from a few metres to a few hundred metres.



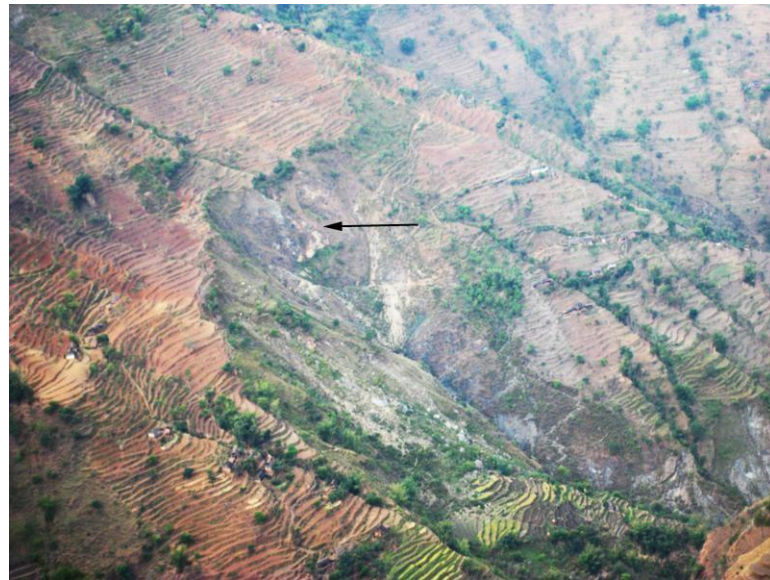
- Hilepani
- Village
- OW 19
- Location points
- River
- Landslides

Figure 2.1 Landslide distribution map with location points of fieldwork





***Plate 2.1 Panoramic view of Bhadare Khola rock fall (arrow indicates the main scarp)***



***Plate 2.2 Landslide below the Ragapur village (arrow indicates the main scarp of the slide)***



***Plate 2.3 Landslide on the right bank of Bhalu Khola ( arrow indicates the main scarp of the slide)***



***Plate 2.4 Landslide in mid reach of Binas Khola (arrow indicates the main scarp of the slide)***





*Plate 2.5 Landslide southeast of Simlebesi (arrow indicates the right flank of the slide)*



*Plate 2.6 Landslide in upper reach of the Bhadare Khola (arrow indicates the main scarp of the slide)*

## **CHAPTER THREE**

### **GEOLOGY OF THE STUDY AREA**

The Himalaya was evolved as a result of collision between northwards moving Indian Plate and the Eurasian Plate. The collision led to a large crustal shortening, accomplished by the orogenic process of the Himalaya. The present-day continuation of the orogeny in the Himalayan belt is evidenced by the occurrence of intense seismic activities in the Himalaya and continued northwards movement of the Indian Plate at a rate of about 5 cm per year (Seeber and Armbruster, 1981; Jackson and Bilham, 1994; Pandey et al., 1995). Most of the convergence is accommodated within the Himalaya by movement on various thrusts and folds (Upreti, 1999).

#### **Regional Geology**

Tectono-morphologically, the whole Himalaya can be divided into different longitudinal units, each having unique stratigraphic and evolutionary characteristics (Gansser, 1964). From south to north, these units are the Terai, Sub-Himalaya (Siwalik), Lower or Lesser Himalaya, Higher Himalaya and the Tethys Himalaya (Figure 3.1). The Pleistocene to recent alluvial deposit covers the southernmost tectonic unit i.e. the Terai zone. It is the Himalayan foreland basin separated by Himalayan Frontal Thrust (HFT) from the Sub-Himalaya. Composed of fluvial deposits of the middle Miocene to early Pleistocene age, the Siwalik or the Sub-Himalaya is bounded by HFT in south and Main Boundary Thrust (MBT) in the north. The Main Central Thrust (MCT) in north and the MBT in south bound the meta-sediments of the Lesser Himalaya. The Higher Himalayan Crystalline rocks overlie the Lesser Himalaya along the MCT. The South Tibetan Detachment System (STDS) separates the medium to high grade metamorphic Higher Himalayan rocks from the overlying low-grade sedimentary rocks of the Tethys Himalaya.

Though these zones are approximately parallel to each other and extend along the Himalayan range, owing to the tectonic and geomorphological processes, a number of nappe, klippe and windows are scattered among these tectonic units.



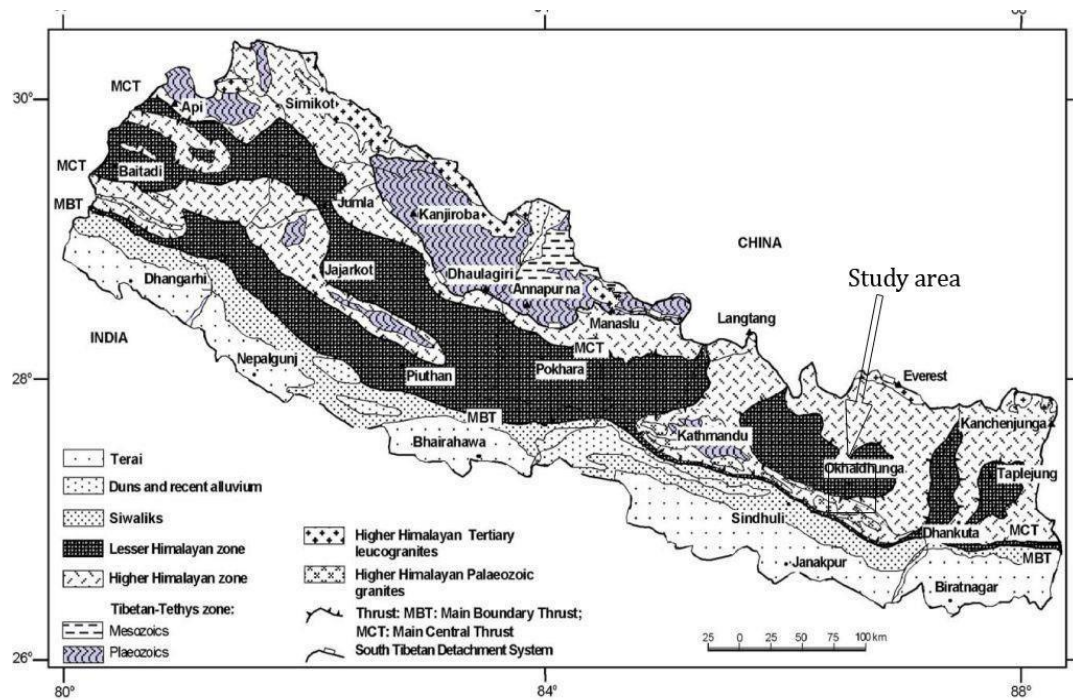


**Figure 3.1** Generalised geological map of Nepal showing the present study area (modified after Amatya and Jnawali, 1994)

### Previous Work in the Study Area

To date only a few geological investigations have been carried out in the present study area. An effort is made to summarise the findings and conclusions of works carried out in the area.

Lombard (1952) introduced the term 'dalle du Tibet' (or Tibetan Slab) in the geological literature for the Higher Himalayan Succession. While describing the eastern Nepal Himalaya, Lombard (1953a, b) made geological cross-section across Mount Everest, Okhaldhunga and the Sun Kosi where the rocks of the Nawakot Nappe surrounded the rocks of the Kathmandu Nappe. Later, another cross-section across Solu Khumbu and the Sun Kosi was prepared by Lombard and Bordet (1956) where the rocks of the Nawakot Nappe were surrounded by the rocks of the Kathmandu Nappe.

Ishida and Ohta (1973) mapped the area between the Tama Kosi River and the Dudh Kosi River and divided the area into the Himalayan Gneisses (Precambrian age), Midland Metasediment Group (Eocambrian age) and Siwalik Series of rocks

(Tertiary age). They also gave the concept of two MCT: the Lower MCT and the Upper MCT. The present study area lies in the Mahabharat Zone, Sun Kosi Tectonic Zone, Ramechhap–Manebhanjhyang Phyllite–Limestone Zone and Okhaldhunga Phyllite Zone. Structurally, the study area includes the Sun Kosi Faults I and II, Vichalo Fault, Dudh Kosi Thrust and Okhaldhunga Anticline and other synclinal and anticlinal folds.

Schelling (1992) carried out a geological research in eastern Nepal between the Sikkim border in the east and the Kathmandu valley in the west and divided the eastern Nepal Himalaya into three distinct thrust-bound tectonic packages; the Higher Himalayan Crystallines, the Lesser Himalayan Thrust Sheet composed of the Lesser Himalayan Series, and the Sub-Himalayan imbricate zone composed of sedimentary rocks belonging to the Siwalik Group. The present study area generally lies in the Ramechhap Group of the Lesser Himalayan Series and Mahabharat Crystalline of the Higher Himalayan Crystallines. The Ramechhap Group of rocks, are comparable to the Nawakot Complex of Stöcklin (1980), which in central Nepal includes the Dhading Dolomite, and thus are believed to be of Precambrian to early Paleozoic age. The Mahabharat Crystalline is roughly comparable to the Bhimphedi Group of Stöcklin (1980) and is considered to be of Precambrian to Cambrian or Ordovician age. Major structures falling in the present study area are the Sun Kosi Thrust and the Okhaldhunga Antiform.

Shrestha et al. (1984) compiled the geology of the eastern Nepal and published a compiled map from the Department of Mines and Geology (DMG). The rocks of the area are divided into the Midland Group and the Kathmandu Group of rocks, separated by the MCT. The Midland Group is further divided into the Ulleri Formation, Kushma Formation, Seti Formation, Naudanda Formation, Ghan Pokhara Formation, Galyang Formation, Sangram Formation, Syangja Formation, Lakharpata Formation and the Takure Formation in ascending order. Similarly the rocks of the Kathmandu Group are divided into the Dware Kharka Schist, Panglema Quartzite, Himal Gneiss, Shiprin Khola Formation, Udaipur Formation, Maksana Formation, Tawa Khola Formation, and Sarung Khola Formation in ascending order. The present study area lies in the Seti Formation of the Midland Group and the Shiprin Khola Formation of the Kathmandu Group.

Dwivedi and Aryal (1997) mapped the area between the Sunkoshi River and the Kakaru Khola dividing the area into the four broad groups of rocks: Low-grade metamorphic rocks of the Lesser Himalaya, i.e. the Nawakot Complex (Stöcklin and Bhattarai, 1977); High-grade metamorphic rocks of the Lesser Himalayan Crystalline, i.e. the Kathmandu Complex (Stöcklin and Bhattarai, 1977); rocks, including volcanic, belonging to the Gondwana sequence; and the Siwaliks. The present study area lies in the low-grade metamorphic rocks (the Kuncha Formation and the Benighat Slates) and the high-grade metamorphic rocks. The major structures lying in the study area are the Mahabharat Thrust and the Sunkoshi Thrust (Sun Kosi Fault II of Hashimoto et al., 1973).

Dhital (2005) mapped the area from Diktel to Hilepani during the engineering work of the Hilepani–Diktel road alignment and divided the area into Banded Gneiss and Garnet Schist unit of Higher Himalaya and Grey Dolomite, Dark grey Schist, Green-purple Phyllite units of the Lesser Himalaya. A part of the present study area lies in the Green-purple Phyllite and Grey Dolomite unit of the Lesser Himalaya and the Banded Gneiss unit of the Higher Himalaya separated by the MCT.

### **Stratigraphy of the Study Area**

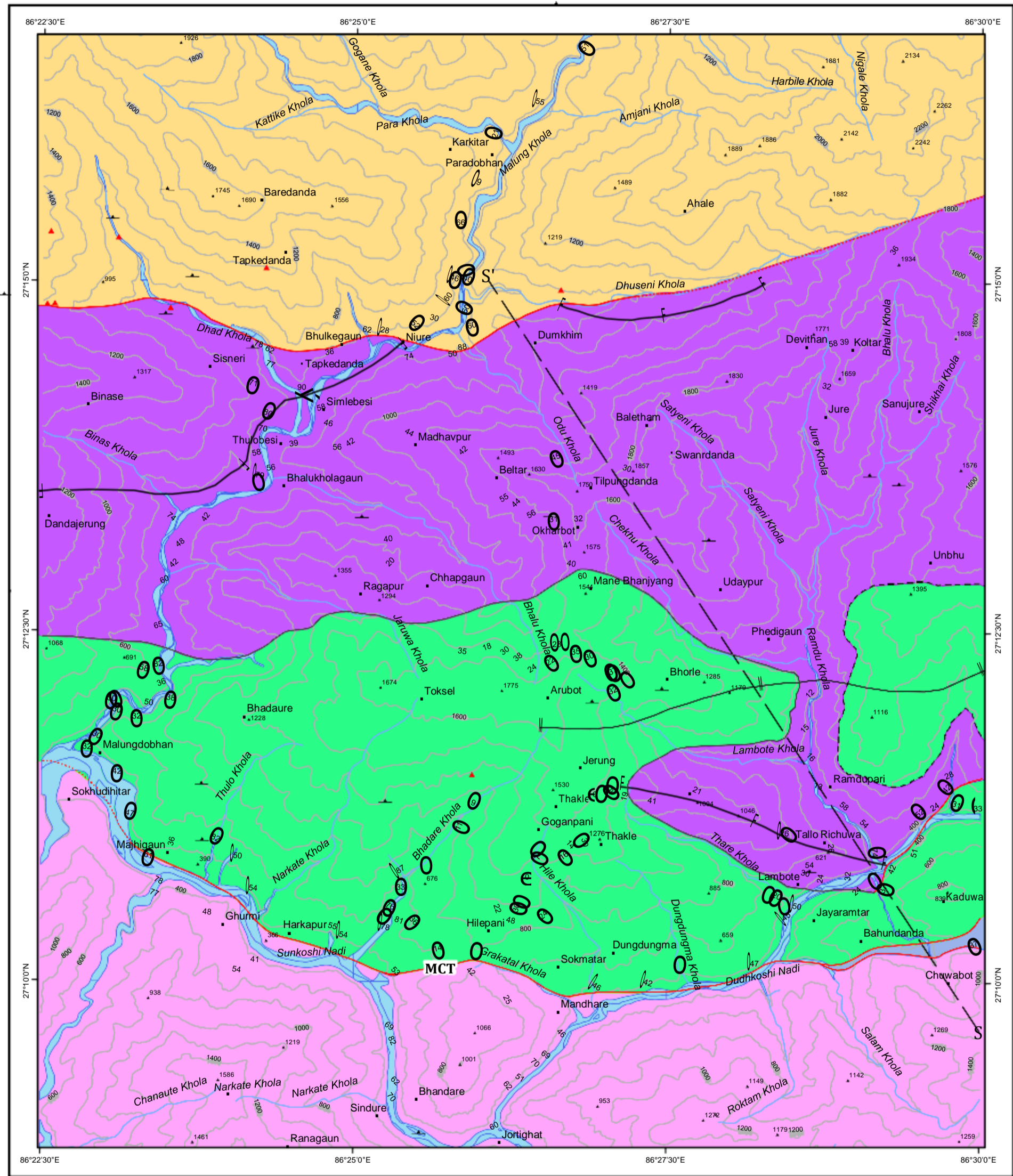
The study area lies in the southern flank of the Okhaldhunga window where the Lesser Himalayan rocks are exposed due to erosion of the Higher Himalayan Thrust sheet. In the region, the Lesser Himalayan rocks are observed north of the Higher Himalayan rocks unlike normal cases where the Higher Himalayan rocks are exposed north of the Lesser Himalayan rocks. The Higher and Lesser Himalayan rocks are separated by the MCT.

The study area can be broadly separated and described as two units.

#### **The Lesser Himalayan Sequence and The Higher Himalayan Crystallines**

The Lesser Himalayan Sequence represents metasedimentary to low grade metamorphic rocks like shale, sandstone, quartzite, phyllite, slate, dolomite and bands of amphibolites. It is divided into four geological formations viz. the Para

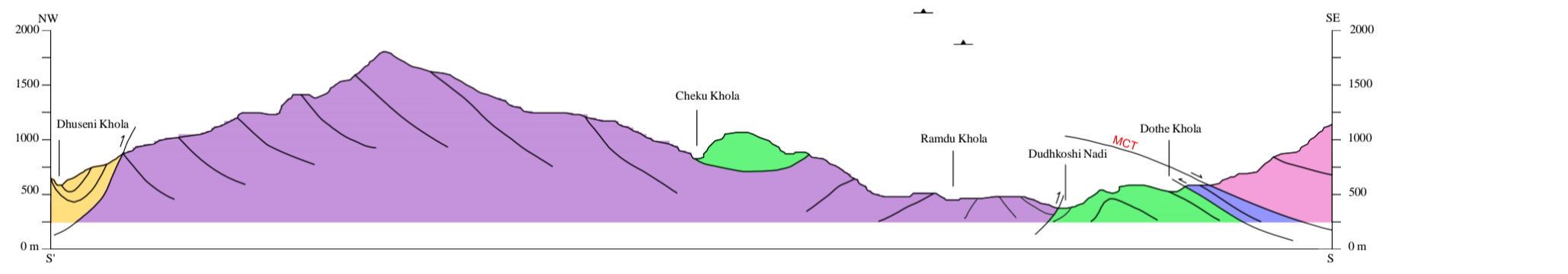




Map Prepared by: Gyawali, B.R., Bijukchhen, S., 2011



- |                       |                  |                |                                  |                         |                               |
|-----------------------|------------------|----------------|----------------------------------|-------------------------|-------------------------------|
| 1586                  | Spot Height      | O              | Bedding                          | <b>Geological units</b> |                               |
| Hilepani              | Village          | +              | Foliation                        | [Green Box]             | Harkapur Formation            |
| [Blue Line]           | Rivers           | e              | Horizontal bed                   | [Purple Box]            | Madhavpur Slates              |
| [Black Line]          | Contour          | <              | Vertical bed                     | [Blue Box]              | Halesi Dolomite               |
| [Black Line]          | Normal contact   | S' - S         | Line of geological cross-section | [Yellow Box]            | Para Khola Formation          |
| [Dashed Black Line]   | Inferred contact | [Red Triangle] |                                  | [Pink Box]              | Higher Himalayan Crystallines |
| [Red Triangle]        | Thrust           |                |                                  |                         |                               |
| [Red Dotted Triangle] | Inferred thrust  |                |                                  |                         |                               |
| [F-F-F]               | Anticline        |                |                                  |                         |                               |
| [H-H-H]               | Syncline         |                |                                  |                         |                               |



Geological cross-section along S'S

Figure 3.2 Geological map of the Ghurmi-Dhad Khola area, Eastern Nepal

Khola Formation, Halesi Dolomite, Madhavpur Slates and Harkapur Formation. The Higher Himalayan Crystallines consist of high-grade metamorphic rocks like schists, gneiss and quartzites (Table 3.1). The units are shown in the geological map of the area (Figure 3.2).

**Table 3.1 Stratigraphy of the Ghurmi–Dhad Khola area**

Rock Units	Formation	Main Lithology	Thickness
Higher Himalayan Crystallines	Higher Himalayan Crystallines	psammatic schist, pelitic schist, banded gneiss, augen gneiss, granitic gneiss, interfingering granite intrusions and quartzite	>1800 m
-----Main Central Thrust-----			
Lesser Himalayan Sequence	Harkapur Formation	greenish-grey calcareous phyllite, slates, siliceous dolomite, light-grey to pink quartzite and amphibolites	>1200 m
	Madhavpur Slates	dark grey to black graphitic slate, with light to dark grey carbonate bands	>1300 m
	Halesi Dolomite	grey dolomite	>200 m
	Para Khola Formation	red-purple quartzite, sandstone, red-purple and green mottled shale with amphibolites	>1000 m

### **Lesser Himalayan Sequence**

The Lesser Himalayan sequence can be further divided into the following formations.

#### ***Para Khola Formation***

The Para Khola Formation is named after the Para Khola where it is well exposed. The unit extends north from the Dhad Khola and Dhuseni Khola and consists of red-purple quartzite, sandstone, red-purple and green mottled shale

with amphibolites. The study area consists of the lower part of the formation. The thickness of the formation is more than 1000 m.

The formation rests upon the younger Madhavpur Slates above a thrust passing along the Dhad Khola (Dhad Khola Thrust). Just above the thrust i.e. at the lower part of the the Para Khola Formation, on the left bank of the Dhad Khola bend near a small landslide (Location WPT 72, in Figure 2.1), grey-green amphibolites, red-purple slate and pink coarse-grained thick quartzite are observed. The general attitude of the rocks is  $106^{\circ}/78^{\circ}$  S.

The major lithotype of the formation on the both banks of the Malung Khola is the highly undulating thick beds of medium- to coarse-grained, cross-laminated, pink to purple quartzite with sporadic purple and green slate partings. Though the formation is right-way-up dipping towards north, due to intense folding, the attitude of beds often abruptly changes in every few 10 metres (Plate 3.1).



***Plate 3.1 Folded rock of the Para Khola Formation (photo taken facing northeast)***

On the uphill side of the foot trail from the Dhad Khola to Niure (WPT 67) grey, grey-green and pale yellow, medium-grained quartzite with grey and green-grey slate partings or beds are observed. The average attitude of the beds is  $132^{\circ}/52^{\circ}$  N.



On the left bank of Malung Khola, about 100 m upstream from the confluence of the Dhuseni Khola and the Malung Khola (Location X 1 in Figure 2.1), medium- to thick-banded medium-grained pink to purple quartzites are observed with general attitude of  $109^{\circ}/40^{\circ}$  N.

On the right bank of Malung Khola on the left abutment of the Para Khola bridge (WPT 60), thinly interbanding of dark grey to grey-green slate and quartzite are oriented at  $14^{\circ}/21^{\circ}$  N.

This formation is comparable to the Nourpul Formation of the Lower Nawakot Group in Central Nepal (Stöcklin and Bhattarai, 1977).

### ***Halesi Dolomite***

This small band of grey dolomite was probably carried all the way from the east by the action of MCT and is seen only in the southern part of the study area. This irregular band has been traced from the Halesi of the Khotang district to Kaduwa of the study area by Dhital (2005) hence is named the Halesi Dolomite. The band appears more or less parallel to the MCT between the Kaduwa and Chuwabot villages and pinches out at Bahundada. The general attitude of the formation is  $68^{\circ}/37^{\circ}$  S (DJ 45). Since this unit was carried all the way from the east by the movement of the MCT, it is separated by the MCT itself from the Higher Himalayan Crystallines rocks and by another thrust from the Harkapur Formation. The formation is more than 200 m thick.

This formation can be correlated to the Dhading Dolomite of the Central Nepal (Stöcklin and Bhattarai, 1977).

### ***Madhavpur Slates***

Well-revealed around the Madhavpur village and thus the name, this unit predominately consists of dark grey to black graphitic slates, though light to dark grey carbonate bands are also not rare. The characteristic feature of the formation, the dark colour of the slates, can be seen in the fresh outcrops along the river or in the road section (Plate 3.2) but is rather difficult to manifest in the weathered exposures as the apparent colour is much lighter.



***Plate 3.2 Graphitic slate of the Madhavpur Slates exposed at Ramdu Khola (picture taken facing west)***

The Madhavpur Slates cover a large extent of the study area: from the Dhad Khola to Chhauri Khahare Khola on the west and from the Dhuseni Khola to Jayaramtar on the east. But the study area does not cover its lower part in the eastern region. This formation is separated from the older Para Khola Formation by the Dhad Khola Thrust to the north and gets transitionally changed to younger Harkapur Formation on the south but shows a sharp contact i.e. a fault contact in the Dothe Khola on southeast part of the study area. This unit can be well observed along the Malung Khola, Ramdu Khola and around Koltar, Baletham, Madhavpur, Ragapur, Okharbot and Richuwa. The thickness of this formation is more than 1300 m.

The lower part of the Madhavpur Slates consist mainly of parallel-laminated dark grey to black graphitic slates with abundant disrupted quartz veins. These slates are exposed in the Dhad Khola (WPT 69, Figure 2.1) where the foliation is almost vertically trending due  $63^{\circ}$ .

On the uphill side of the road from Devithan to Ketuke, north of Koltar (OW 88) thinly laminated and foliated light to dark grey graphitic slate with disrupted quartz veins are observed. The attitude of foliation is  $79^{\circ}/31^{\circ}$  S. Similar lithotype



was also observed on the uphill side of the road to the northeast of Baletham, with the foliation orientation of  $102^{\circ}/44^{\circ}$  S (OW 93).

The middle part of the unit comprises dark grey to black graphitic slates with bands of grey calcareous rocks in between the slates. On the uphill side of the foot trail from the Dhad Khola to Malungdobhan, above a large concave bend of the river (WPT 73), thin interbedding of grey-green to dark-grey slate and dark grey dolomite are observed. The average attitude of the beds is  $114^{\circ}/80^{\circ}$  N. Thinly to medium-bedded light to dark grey laminated dolomite with dark slate partings are observed near the Jure village along the newly dug road from Koltar (OW 91). The beds were oriented at  $105^{\circ}/37^{\circ}$  S.

The upper part of this unit also has the black graphitic slates but the calcareous beds are somewhat rare. On the uphill side of the foot trail from Dhad Khola to Malungdobhan, right bank of the Malung Khola (WPT 78), medium to thick bands of dark grey to black, frequently laminated slates and sporadically calcareous siltstone are observed. The attitude is  $61^{\circ}/60^{\circ}$  S. Thinly foliated dark grey to black slates with foliation of  $94^{\circ}/26^{\circ}$  S with few bands of carbonate rocks are observed on the uphill side of the road from Manebhanjyang to Ragapur (OW 117).

On the right bank of the Ramdu Khola about 300 m downstream from the confluence with the Cheku Khola (OW 46), thin-banded, deformed black slates with quartz veins parallel to foliation are observed. The foliation has an attitude of  $44^{\circ}/12^{\circ}$  N.

The Madhavpur Slates has a transitional contact with the Harkapur Formation except for the eastern part where the contact is a fault. The contact passes through the Chhauri Khahare Khola on the east, through the saddle between Manebhanjyang and Okharbot and along the Cheku Khola, Thare Khola and Dudhkoshi on the east.

The unit generally exhibits steep foliations on the west but it gradually changes to gentle dips to the east where the rock beds are almost horizontal. The graphitic slates are well exposed in the Ramdu Khola but the younger rocks of

the Harkapur Formation are seen just a few hundred metres above in the cliffs on both sides of the river.

The formation is folded and a couple of large anticlines trending northeast-southwest and northwest-southeast and a syncline trending east-west can be noticed.

By the lithostratigraphy and character of the rocks the formation can be correlated with the Benighat Slates of Upper Nawakot Group in Central Nepal with the calcareous beds comparable with the 'Jhiku Member'.

### ***Harkapur Formation***

The formation is well exposed around the Harkapur village and is characterised by a mixed lithology of greenish-grey calcareous phyllites, slates, siliceous dolomites, light-grey to pink quartzite and amphibolites. Generally it is more intensely deformed at the upper or the southern part than in the lower part due to the movement related to the MCT. The dolomite and slates of the Harkapur Formation differ from those of the Madhavpur Formation in that their colour is somewhat greenish-grey. The rocks of this formation can also be observed at Toksel, Manebhanjyang, Bhorle, Kaduwa, Jayaramtar and Hilepani. The thickness of the formation is more than 1200 m.

Separated from older rocks of the Madhavpur Slates by a transitional contact, the Harkapur Formation is separated by MCT from the Higher Himalayan rocks and by another thrust from the Halesi Dolomite.

An outlier structure of the formation can be observed in the Lukapani village where the underlying slates are exposed in the Ramdu Khola and the dolomite and phyllite of the Harkapur Formation are apparently exposed on the hill-top.

The lower part of the Harkapur Formation consists of light grey medium- to thick-bedded dolomite with interbanding of grey, green-grey to dark-grey slates. It can be observed on the uphill side of the foot trail from Dhad Khola to Malungdobhan above the suspension bridge over the Malung Khola north-west of the Chhuri Khahare dobhan (WPT 79, Figure 2.1). The beds are oriented at 82°/82° S. A similar lithotype is exposed in the upper section of the road from

Hilepani to Manebhanjyang, about 400 m south of Manebhanjyang (WPT 46) and the rocks display a general attitude of  $65^{\circ}/37^{\circ}$  S.

On the right bank of the Sodhu Khola about 200 upstream from its confluence with the Dudhkoshi (OW 42), the outcrop consists of deformed medium- to thick-bedded light grey dolomite with partings of greenish-grey phyllite. The attitude of the dolomite beds is  $43^{\circ}/42^{\circ}$  N.

The middle part of the unit consists of greenish-grey phyllite, light grey to green-grey calcareous parallel-laminated quartzite with grey-green phyllite or slate partings and some thick beds of light grey to white dolomite. The dolomite and quartzite are medium- to fine- grained. This lithotype can be clearly observed near the Malungdobhan (WPT 81), along the wall of the canal at the left bank of the Manlung Khola. The quartzite bands have an attitude of  $101^{\circ}/50^{\circ}$  S. Similarly the interbanding of dolomite and quartzite can also be seen at Jerun village.

The upper part of the Harkapur Formation is shattered. It has typical interbanding of greenish-grey calcareous phyllite and greenish-grey araneous dolomite (Plate 3.3).

On the Bhadare Khola section the outcrops consist of light grey highly deformed thin-bedded white dolomite with partings of greenish grey phyllite. Along the foot trail from Majhigau to Malungdobhan at the western end of the Majhigau village (OW 80), thinly bedded, light grey deformed dolomite and thinly foliated, greenish-grey, highly fractured crenulated calcareous phyllite display a general attitude of  $104^{\circ}/61^{\circ}$  S.

About 500 m towards Okhaldhunga from the saddle of Hilepani along the road, greenish-grey calcareous phyllites are observed with some sporadic amphibolite bands. About 200 m towards Okhaldhunga from there the outcrops consist of crenulated, calcareous grey phyllite and grey dolomite with an attitude of  $84^{\circ}/26^{\circ}$  S (WPT 36).

The Higher Himalayan Crystallines cover the uppermost part of the formation and have deformed whatever remained of the upper part.



*Plate 3.3 Typical interbanding greenish-grey phyllite and greenish-grey dolomite at location OW 25 (picture taken facing north)*

Though the unit cannot be compared or correlated with any single lithotype of central Nepal, it can be correlated with the Malekhu Limestone and the Robang Formation, where the former correlates the lower part and the latter the upper.

### **Higher Himalayan Crystallines**

The Higher Himalayan Crystallines lie slightly discordantly over the Lesser Himalayan sequence. They consist of psammitic schist, pelitic schist, banded gneiss, augen gneiss, granitic gneiss, interfingering granite intrusions (Plate 3.4) and a few bands of white quartzite. Separated by the MCT with the Lesser Himalayan rocks, the Higher Himalayan Crystallines are distributed around the Mandhare, Jortighat, Hilepani, Ghurmi and Sokhudhitar villages. This unit is more than 1800 m thick.

Thin- to medium-banded white quartzite with thinly foliated dark grey psammitic to pelitic garnetiferous schist is observed on the right bank of

Bahadur Khola, 50 m upstream from the suspension bridge over the river (OW 82, Figure 2.1). The quartzites are oriented at  $112^{\circ}/77^{\circ}$  S.



*Plate 3.4 Granitic intrusion in the Higher Himalayan Crystallines at OW 18 (photo taken facing north)*

On the right bank of the Sunkoshi river, 10 m downstream from the right abutment of an under-construction bridge over the Sunkoshi (OW 87) the outcrop consists of medium- to thick-banded, coarse-grained, light grey psammitic schist with partings of pelitic schist. The schists contain garnets and deformed quartz veins parallel to foliation. The psammitic schists exhibit gneissic texture; and the general attitude of the foliation is  $95^{\circ}/41^{\circ}$  S.

On a small stream east of Ghurmi (OW 86), medium to thick banded augen gneiss with augens of feldspar, quartzite (tourmaline embedded) and a thin band of granitic gneiss is observed.

On the left bank of the Sunkoshi river about 20 m downstream from the confluence of a tributary flowing from the Hilepani school and the Sunkoshi, the outcrop consists of thin to thick bands of garnet-psammitic schist and crenulated pelitic schist.

On the right bank of the Dudhkoshi along the foot trail from Jortighat to Jayaramtar (OW 20), thick-banded augen gneisses with schist partings were

observed. The augens up to 3 cm across are comprised of quartz, feldspar and tourmaline. A 45 cm thick concordant band of granitic gneiss was also observed between the augen gneisses. The average attitude of foliation is  $124^{\circ}/51^{\circ}$  S.

## Geological Structures

The geological structures observed in the study area are classified and described briefly as major and mesoscopic and minor structures.

### Major Structures

The MCT is the dominant major structure of the study area. Apart from the MCT there are two faults and two regional anticlines and a syncline in the area.

#### *Main Central Thrust*

The MCT juxtaposes the crystalline rocks of the Higher Himalaya over the metasedimentary rocks of the Lesser Himalaya (Acharya, 2008). The thrust carries the Higher Himalayan rocks as hanging wall over the Lesser Himalayan rocks or the footwall. In the study area it extends E-W and dips towards the south. The MCT is very distinct in the area and can be demarcated easily. It passes along the Sunkoshi River to the west and continues through the saddle of Hilepani (Plate 3.5) and then along the Dudhkoshi River.

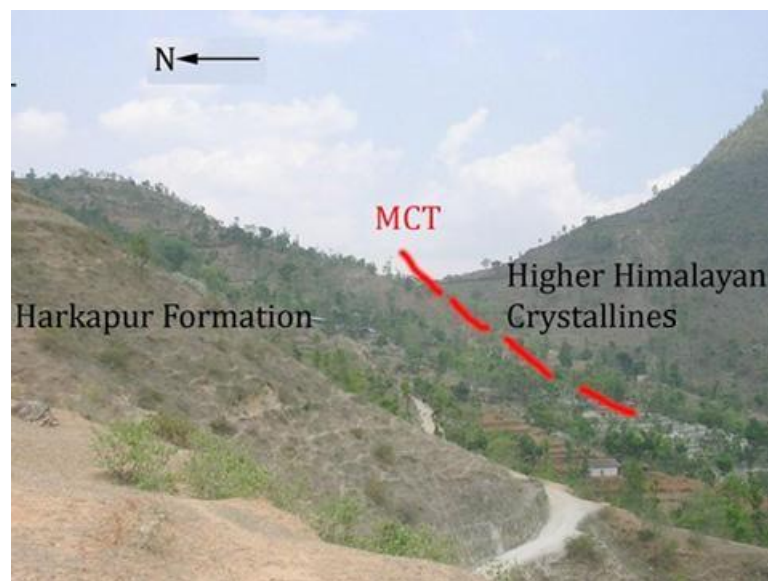


*Plate 3.5 Position of the MCT at the saddle of Hilepani*

At the Hilepani saddle the distinct metamorphic break suggests the position of the MCT. It separates the Higher Himalayan Crystallines with the Harkapur Formation of Lesser Himalaya to the west and centre and with the band of Halesi Dolomite to the east of the area.

Since the study area is the southern part of the Okhaldhunga window, the MCT separates the south lying Higher Himalayan Crystallines from the north lying Lesser Himalayan sequence.

### ***Dhad Khola Thrust***

The E-W trending and north-dipping Dhad Khola Thrust separates the older Para Khola Formation and younger Madhavpur Slates. It is observed in the north part of the area and passes through the Dhad Khola and Dhuseni Khola. The thrust is lineated based on the contrasting lithology in its hanging wall and footwall. The folds observed in them are discordant, but there is indistinct shear or crushed zone.

### ***Faults***

A reverse fault is observed in the southeast study area (OW 34 and 35) where it separates the Madhavpur Slates and the Harkapur Formation. Even though these two formations have a transitional boundary almost all over the study area, there is a NE-SW trending thrust contact at the eastern part.

The Halesi Dolomite is separated from the Harkapur Formation by another thrust. This south-dipping reverse fault is more or less parallel to the MCT. Though it extends a long way to the east of the study area, it is truncated by the MCT in the southeast part of the study area.

### ***Anticlines and Synclines***

A couple of anticlines and a syncline are observed in the study area. In the northwest part of the area a NE-SW trending anticline is observed in the Madhavpur Slates.

An E-W trending syncline in Harkapur Formation is observed in the southeast. It passes through the Bhorle village but its extension towards the west is not observed.

Another anticline is observed just south of the syncline in the Madhavpur Slates. The anticline has NW–SE trend and is overlain by the thrust separating the Madhavpur and Harkapur Formations.

### **3.4.3 Mesoscopic and Minor Structures**

Several mesoscopic and small-scale structures like folds, foliations, beddings, ripple marks, quartz veins and drag folds are common in the area. The rock units are highly folded and deformed in most part of the study area. Mesoscopic folds (Plate 3.6), ptygmatic folds, drag folds and disrupted quartz veins are very common and numerous. The phyllites of the Harkapur Formation are most deformed. The slates of Madhavpur Formation also contain deformed and disrupted quartz veins (Plate 3.7) at some locations.





***Plate 3.6 Mesoscopic fold observed in the Higher Himalayan Crystallines at OW 22 (photograph taken facing east)***



***Plate 3.7 Disrupted quartz veins in the graphitic slate of the Madhavpur Formation at OW 92 (photograph taken facing northeast)***

## **CHAPTER FOUR**

### **GIS OVERLAYS FOR SUSCEPTIBILITY ANALYSIS**

The main objective of the present study was to prepare landslide susceptibility maps of the Ghurmi-Dhad Khola area, Okhaldhunga. Landslides frequently occur in the area and seriously affect local living conditions. The landslides are also a nuisance for the roads joining the district headquarters of three districts with rest of the country. Hence the demarcation of the landslide susceptible areas helps further the infrastructure and development works in the study area.

For the purpose of landslide susceptibility mapping, different factors are considered. These factors are thought to have a landslide triggering effect. For the susceptibility analysis these factors are depicted in form of thematic maps or the GIS overlays. Apart from these factor maps, a landslide inventory map i.e. map depicting existing landslides was also developed. Before the factors considered for present study are looked into, an attempt to give a general account on the causative factors of landslides is made.

#### **Causative Factors of Landslides**

When the balance of the resisting strength of the soil or rock forming the slope against gravity is tipped in favour of gravity, a landslide occurs. This balance can be changed by both natural and man-made circumstances. The elements that affect slope stability and landslides are numerous and varied, and interact in complex and often subtle ways (Varnes, 1984). The various causative factors of landslides can be described as following.

#### **Geological Factors**

There is an association between geological material and landslide occurrence. The geological causes of landslides can be as follows.

- Extensive development of soft or fractured rocks such as phyllites, slates and schists; presence of calcareous interlayers in these rocks which leads to high porosity and void formation due to leaching and dissolution.
- High weathering of rocks.

- Sheared, jointed or fissured materials, heavily fractured rocks because of intense folding and faulting.
- Adversely oriented discontinuity (bedding, joints, faults, unconformity, contacts etc).
- Contrast in permeability of materials.

### **Morphological Factors**

- Tectonic or seismic activity. The Himalayan Range lies in a high seismicity belt. Several active faults have been mapped. Landslides due to seismic loading are very common.
- Fluvial erosion of slope toe. Undercutting of the banks by deeply incised rivers and streams.
- High relief or steep slopes with slope gradient, slope shape and slope aspect also playing their parts in occurrence of landslides.
- Vegetation removal by natural causes like fire and draught.
- Concentrated precipitation. In the region like ours where maximum precipitation occurs in a period of less than 3 months, the concentrated precipitation is one of the most principal triggering causes of landslide occurrences.

### **Anthropogenic Factors**

- Intense deforestation on the slopes of the hills may trigger landslides.
- Improper land use which includes agricultural practices on steep slopes, irrigation on steep and vulnerable slopes, overgrazing and quarrying for construction material without considering the condition of the terrain.
- Lack of terrain capability evaluation before construction of infrastructure in the hilly areas.

### **GIS Overlays or Thematic Maps for the Present Study**

Taking into account, the above mentioned causative factors of landslides, 9 factors were considered for the present study: geology, distance from faults and folds, distance from drainage, rock and soil type, land cover, slope aspect, slope

angle, altitude and rainfall. Apart from these maps a map showing the distribution of existing landslides was also prepared. Brief description of these overlays is given here.

### **Landslide Inventory Map**

To determine landslide hazard and undertake an estimation of future landslide occurrence, an understanding of the conditions and processes controlling landslides is required (Long, 2008). The landslide distribution map helps in understanding the factors and conditions controlling the landslides and is used as a basis for landslide susceptibility zonation.

Landslide distribution map or inventory map is a spatial distribution of existing landslides of any area. Preparation of landslide inventory map is the most important and initial step for landslide susceptibility analysis. The existing landslides are taken into consideration for predicting and evaluating susceptible areas as future landslides are likely to occur in same geological, hydrological and geomorphic condition as those in the past.

Three main approaches were undertaken for the preparation of the map: study of topological map, interpretation of Google Earth® image and fieldwork. The landslides marked on the topological map of Department of Survey, 1995 were updated by study of the Google Earth® image of 2002 and then were verified and further updated by a series of fieldwork in 2010 and 2011. The demarcation of the landslides on the topographic map was carried out in the field using a GPS. These three approaches were coupled to prepare a reliable landslide distribution map in form of a polygon map (Figure 2.1).

The study area, being a structurally complex terrain, is prone to slope instability due to its lithological and structural characters. The inventory map shows landslides covering 20,688 pixels i.e. an area of 2.069 sq. km (each pixel being 10 m x 10 m in size). A total of 77 landslides were identified and it was observed that the southern part of the study area consisted of more landslides than its other parts.

The landslides are observed in form of clusters, the prominent one being in the Bhadare Khola. Other landslide clusters are observed around the Bhalu Khola, Dothe Khola and around Koltar area. Fragile lithology and deep gulley erosion seems to be main cause of a majority of the slides.

### **Geological Map**

Geology is one of the prime and important causative factors causing slope instability. The geology and geological map of the area is already discussed in Chapter 3.

A simplified geological map extracted from Figure 3.2, was then used for susceptibility analysis (Figure 4.1). Five different lithological units mapped are the Para Khola Formation, Halesi Dolomite, Madhavpur Slates, Harkapur Formation and Higher Himalayan Crystallines. The Para Khola Formation consists of quartzite, sandstone, shale, slate and amphibolite. The Halesi Dolomite is a small band of dolomite whereas predominantly slates with occasional interbanding of calcareous rocks comprise the Madhavpur Slates. The Harkapur Formation is composed of phyllite, dolomite, quartzite and amphibolite. The Higher Himalayan Crystallines has schist, gneisses, granite and quartzite. A majority of the landslides occur in the Harkapur Formation. As mentioned earlier, the Harkapur Formation has fragile and crushed lithology in the upper part and this plays a vital role in the slope instability in the area. Only a portion of the Para Khola Formation lies in the study area and it lacks prominent landslides. It may be due to the competent rocks like quartzite and sandstone.

The Madhavpur Slates and Higher Himalayan Crystallines also share a fair amount of landslides between them. The small area covered by the Halesi Dolomite though contains a prominent landslide which may be due to the deformed lithology sandwiched between the MCT and another thrust. The percentage of total area covered and percentage of landslide occurrence in the units are shown in Figure 4.2.

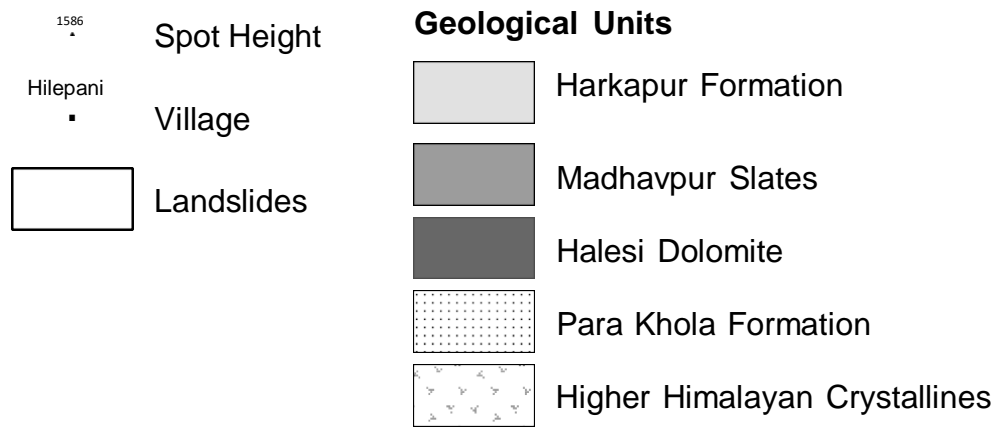
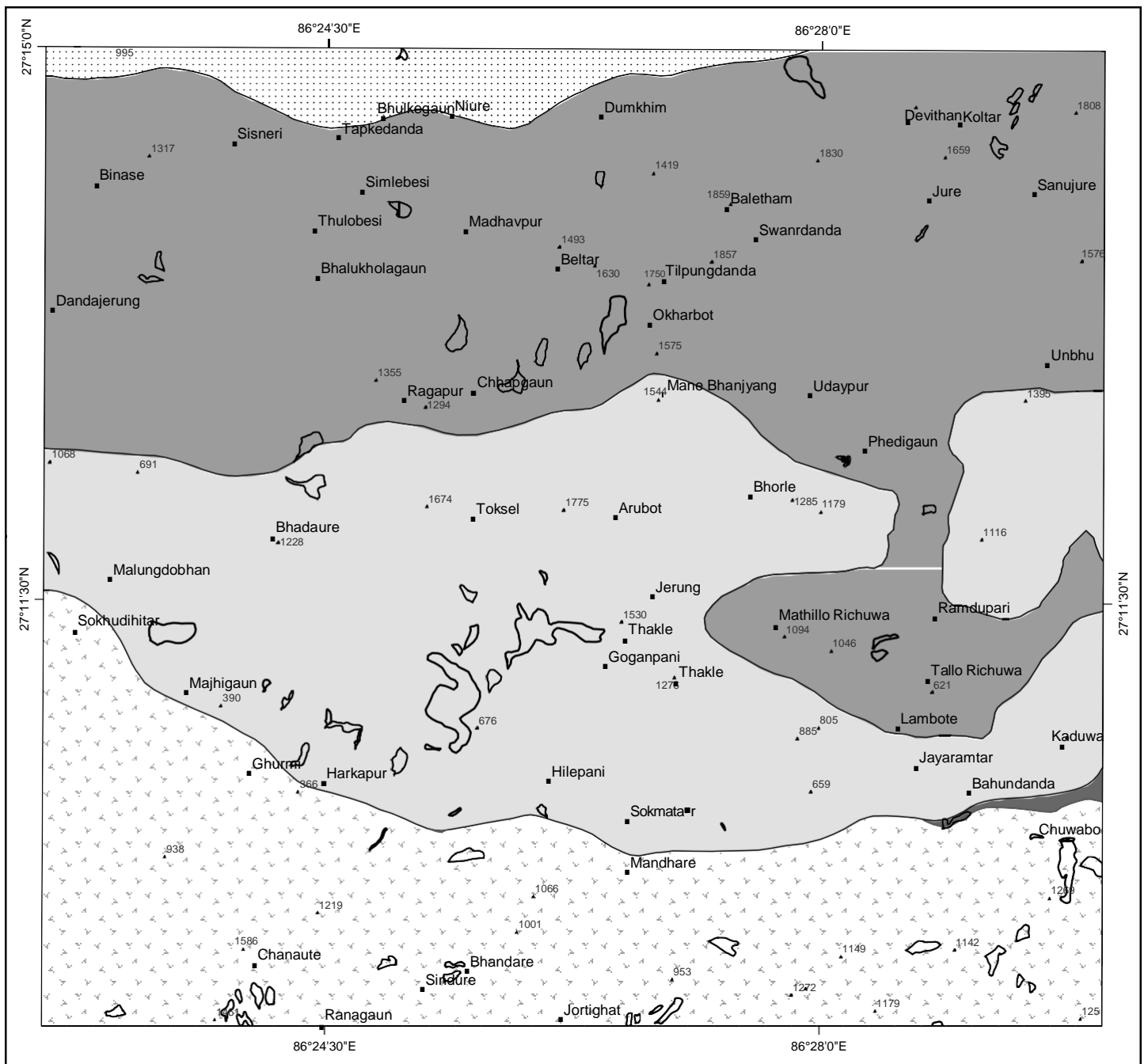
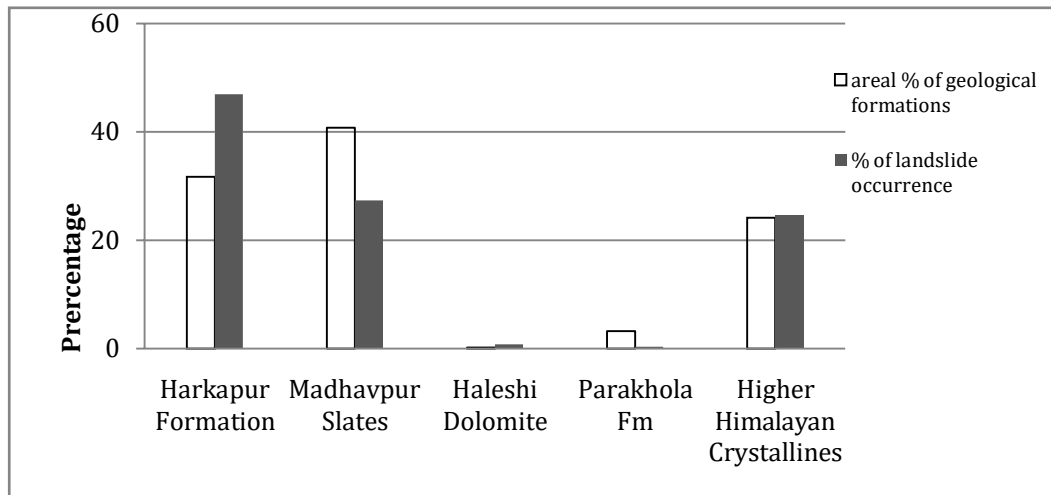


Figure 4.1 Simplified geological map of the study area



*Figure 4.2 Percentage of geological units and landslides occurring in them*

### **Distance from Fault or Fold-axis**

Slope instability is contributed by folding, faulting and fracturing of rocks due to tectonics. Accepting this fact another factor, distance from faults and folds was considered. The folds and faults were extracted from the geological map. The distance from them were calculated using the Euclidean distance tool in the GIS application and then grouped in three continuous classes viz. less than 50 m, 50–100 m and more than 100 m (Figure 4.3). It is theoretically considered that landslides occur near the faults and folds and decreases as the distance increases. But the condition in the study area does not match the case as majority of landslides have occurred more than 100 m away from major fold-faults. It may be inferred that they may not be the prime governing factor in occurrence of landslides in this particular case or the effect of regional thrusts like MCT shows its effect up to distances much farther than 100 m. The following bar diagram (Figure 4.4) shows the relative distribution of landslide percentage in the three classes.

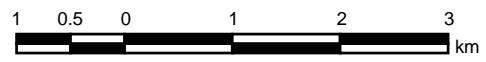
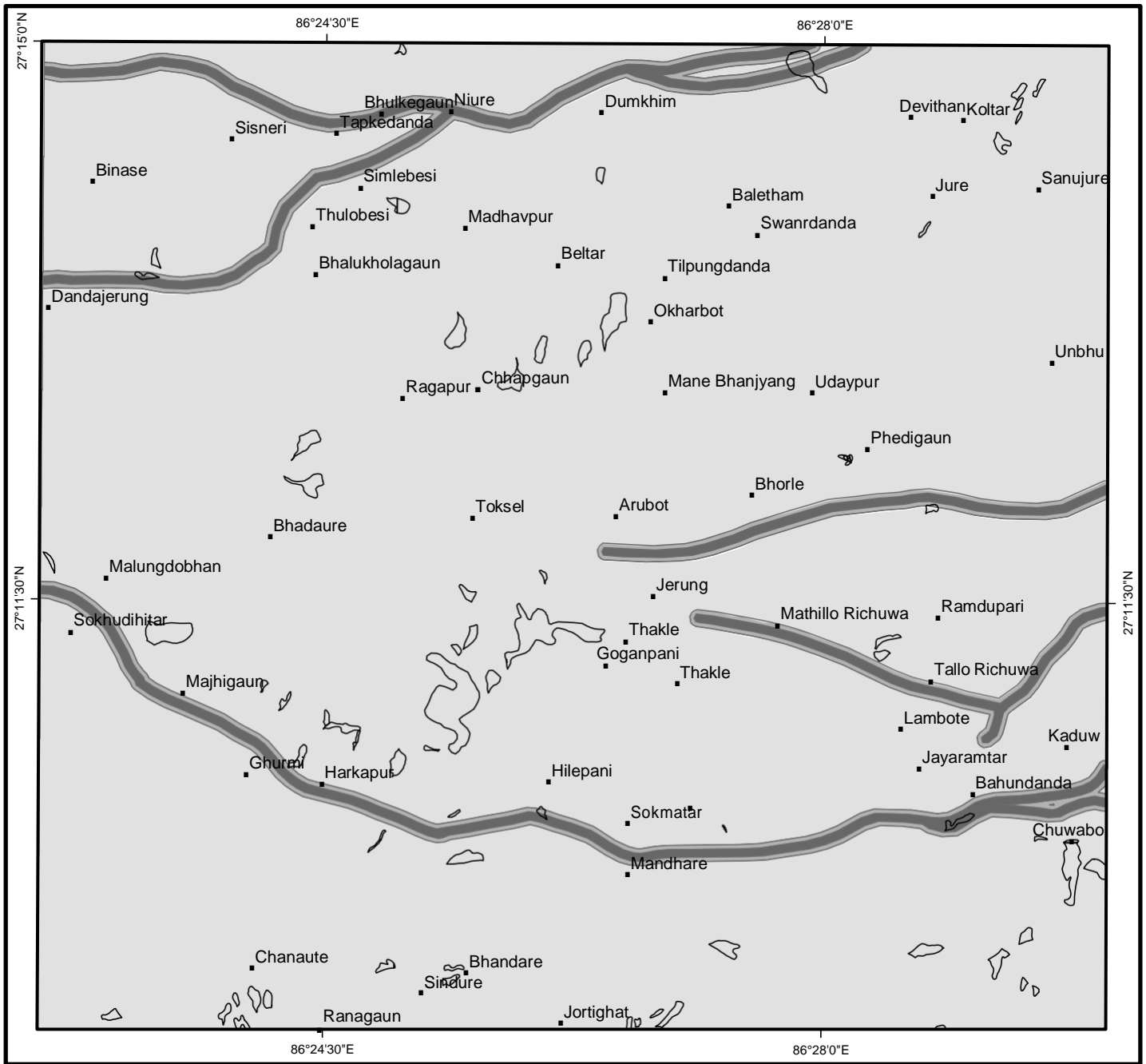


**Figure 4.3** Distance from faults and folds



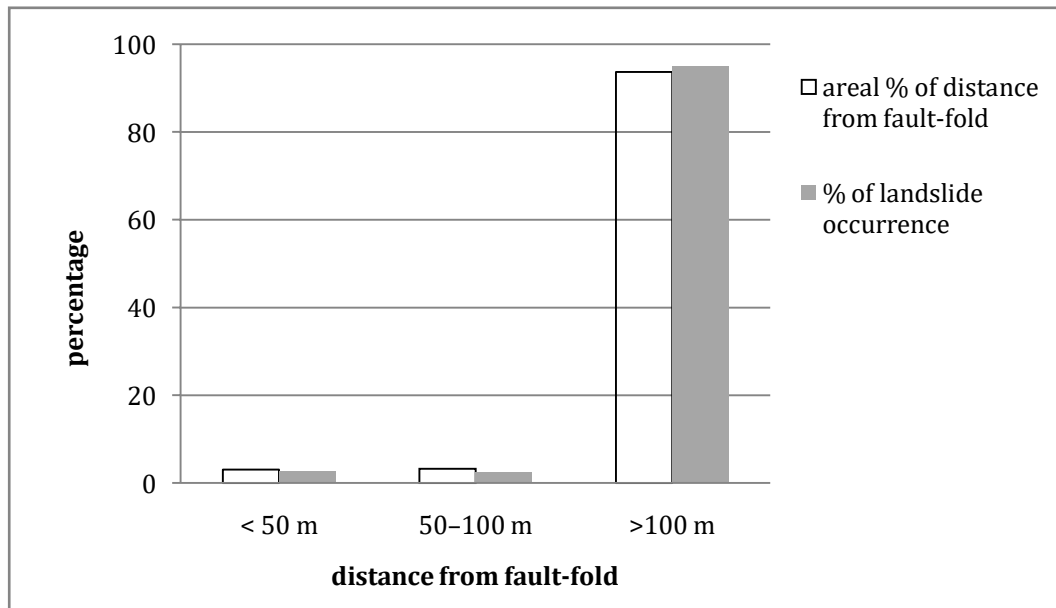


*Figure 4.4 Area covered by distance from fault-fold classes and landslides occurring in them*

### **Distance from Drainage**

To assess the effect of drainage on landslide occurrence the distance from drainage was considered. It is evident from studies that closeness to the streams will have a major effect on landslide occurrence. The intensive gully erosion of the streams is the main cause for the mass wasting to occur. The distance from drainage was calculated by Euclidean distance tool of the GIS application and reclassifying the resultant map into four classes: less than 25 m, 25–50 m, 50–100 m and more than 100 m (Figure 4.5). A majority of landslides do occur in the area less than 50 m away from drainage. The incising action of the streams and deep gully erosions is the major cause of these landslides. The stream density is also higher in the area which adds up to the reasons of the landslides.

The area shows a positive trend in the case of drainage distance and occurrence of landslides i.e. the more nearer a stream the more chance of a landslide to occur. The percentage of landslide occurrence in each of the classes with their areal percentage is tabulated in Table 4.1.

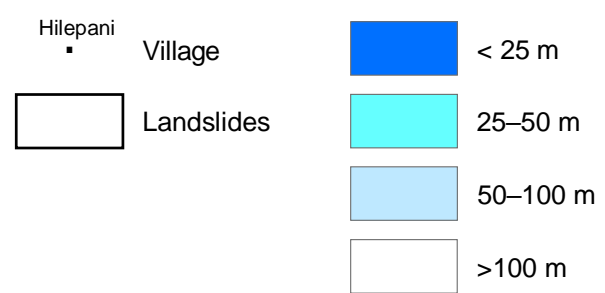
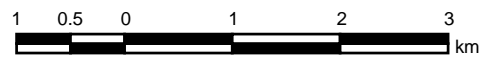
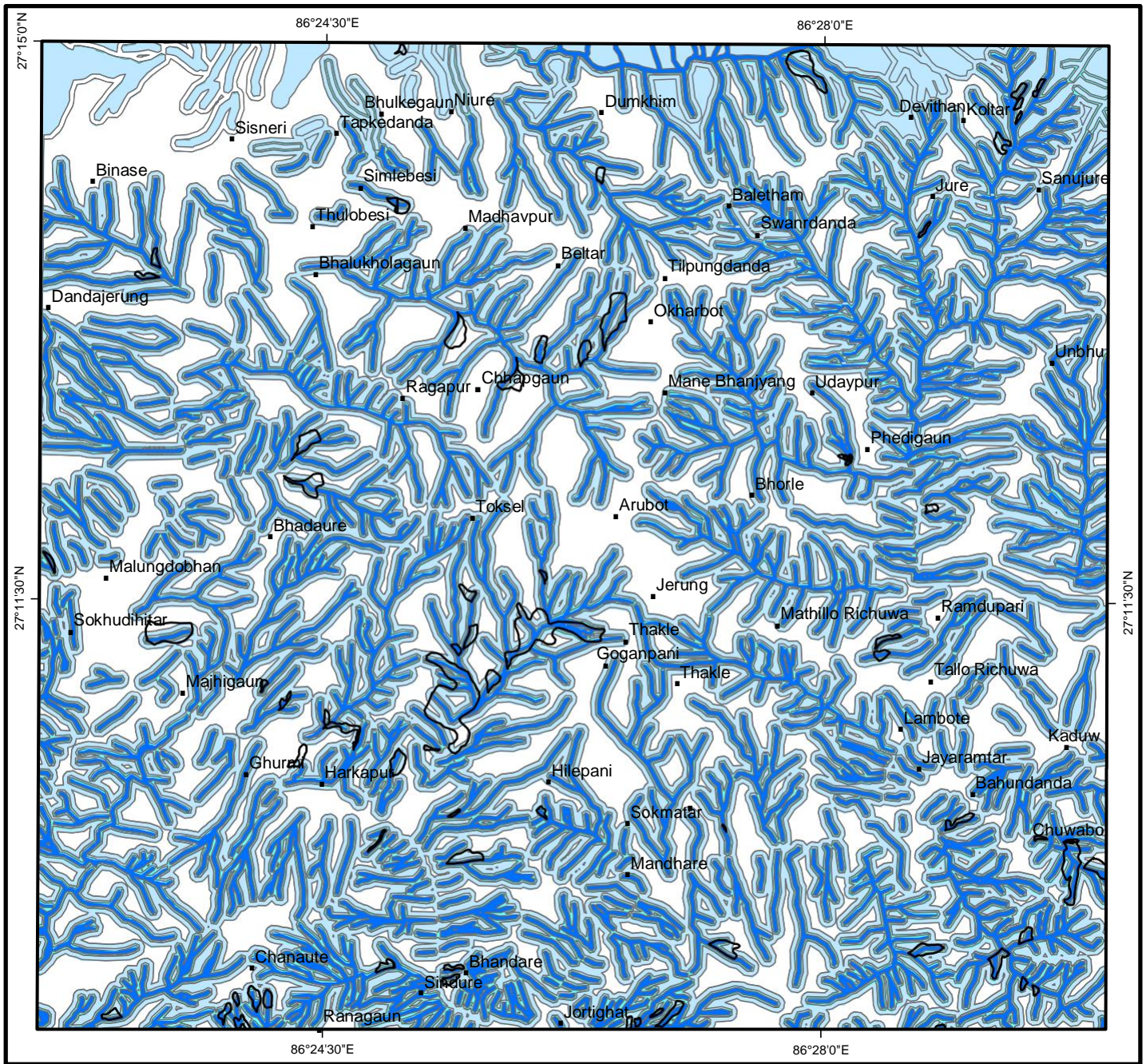


**Figure 4.5 Distance from drainage**



**Table 4.1 Areal percentage of distance from drainage classes and occurrence of landslides in each class**

<b>Distance form drainage</b>	<b>Percentage covered</b>	<b>Percentage of landslide occurrence</b>
< 25 m	22.18	39.05
25-50 m	17.25	23.29
50-100 m	32.09	28.15
> 100 m	28.48	9.51

### **Rock and Soil Distribution**

Rock and soil also has roles in causing surface instability. Strength of rock, strength and depth of soil etc. are responsible for mass movements. So a rock-soil map of the area was prepared with the different classes being rock, shallow residual soil (thickness less than 5 m), thick residual soil (thickness more than 5 m), colluvium and alluvium (Figure 4.6). The classification is based on fieldwork and the data were used to prepare the polygon map in the GIS application. Due to the absence of rock strength test, rock zones were not differentiated according to their strength. A majority of landslides occurred in the colluvial soil. It is apparent as colluvial material lack strength and easily slide down a slope with even an insignificant triggering. The area also has many slides in the rock. The fragile and deformed incompetent rocks with unfavourable joint patterns may be the predominating cause of the rock sliding. The landslide cluster in the Bhadare Khola lies both in colluviums and rock but the landslides in the Bhalu Khola area occur extensively in colluviums. The residual soils are devoid of landslides as they are formed in flat areas. Table 4.2 shows the landslide distribution in each of rock or soil class.

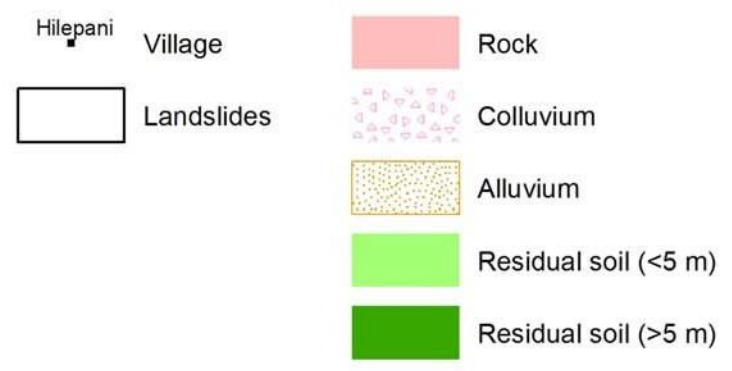
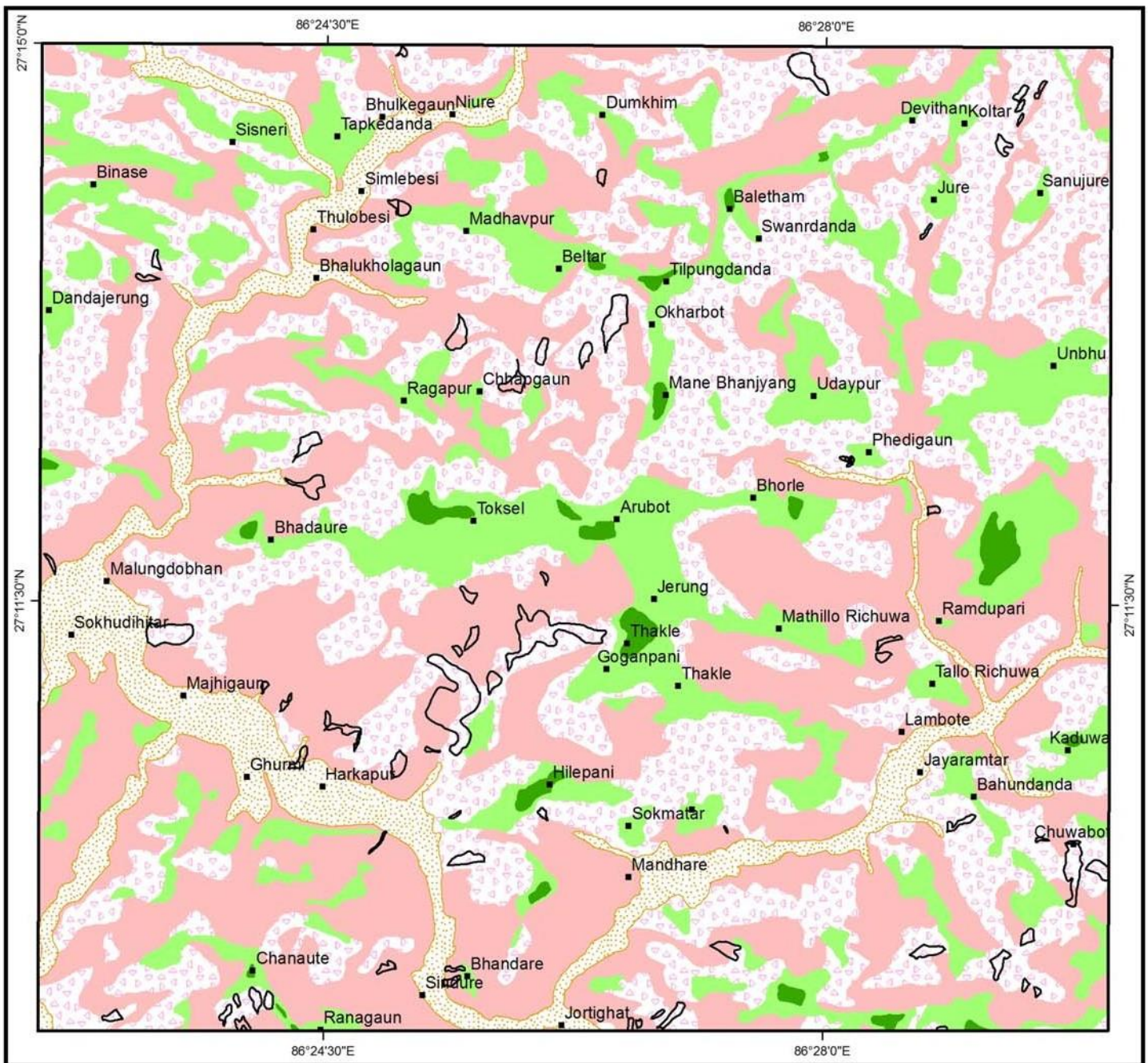


Figure 4.6 Rock and soil distribution map

**Table 4.2 Percentage coverage of rock-soil classes and occurrence of landslides in each class**

<b>Rock and Soil parameters</b>	<b>Percentage covered</b>	<b>Percentage of landslide occurrence</b>
Rock	39.22	34.88
Alluvium	7.72	0.82
Colluvium	34.05	63.56
Residual soil (Shallow, <5 m)	18.09	0.74
Residual soil (Thick, > 5 m)	0.91	0.00

### **Land cover**

Land cover or land use also affect the occurrence of landslides. The land cover map of the area is prepared on basis of topographic map and verified during field work. The polygon map was prepared by classifying the various types of land covers as cultivated and built-up, forest, grassland, bush, sand, water body and barren land (Figure 4.7). More than 90% of the area is covered by cultivated land and forest, each being a little more than 45%. A majority of landslides are found to be in the forest area (Table 4.3). The dense and sparse forests were not differentiated in the study, neither was the cultivated land differentiated into irrigable and non-irrigable. The sparse vegetation i.e. the shrubs may have been more responsible for the landslides than big trees. And, as it is often seen in the study area even though there were big trees in a certain hill-slope, a landslide occurred and it even uprooted and dislodged the trees. It may show that big landslides cannot be controlled by vegetation alone. Cultivated and built-up lands have relatively less landslides than the area it covers as most of these lands are in the flat areas where chances of landslides are less. The bush and grasslands generally develop in crushed and fragile rock hence, they were prone to landslides. It is observed that the landslide occurrence in them is relatively high.



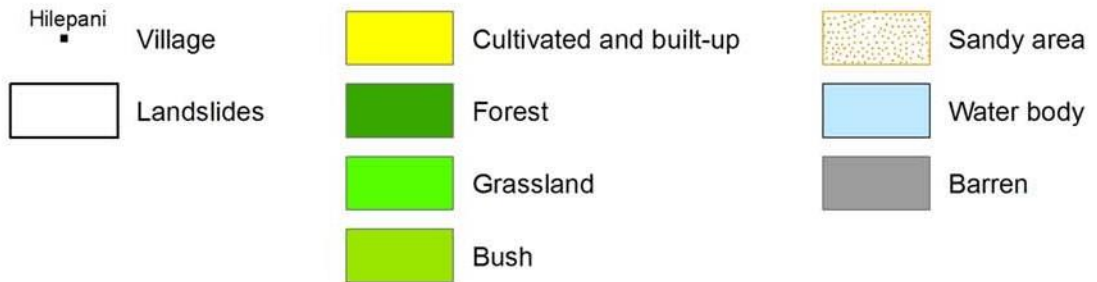
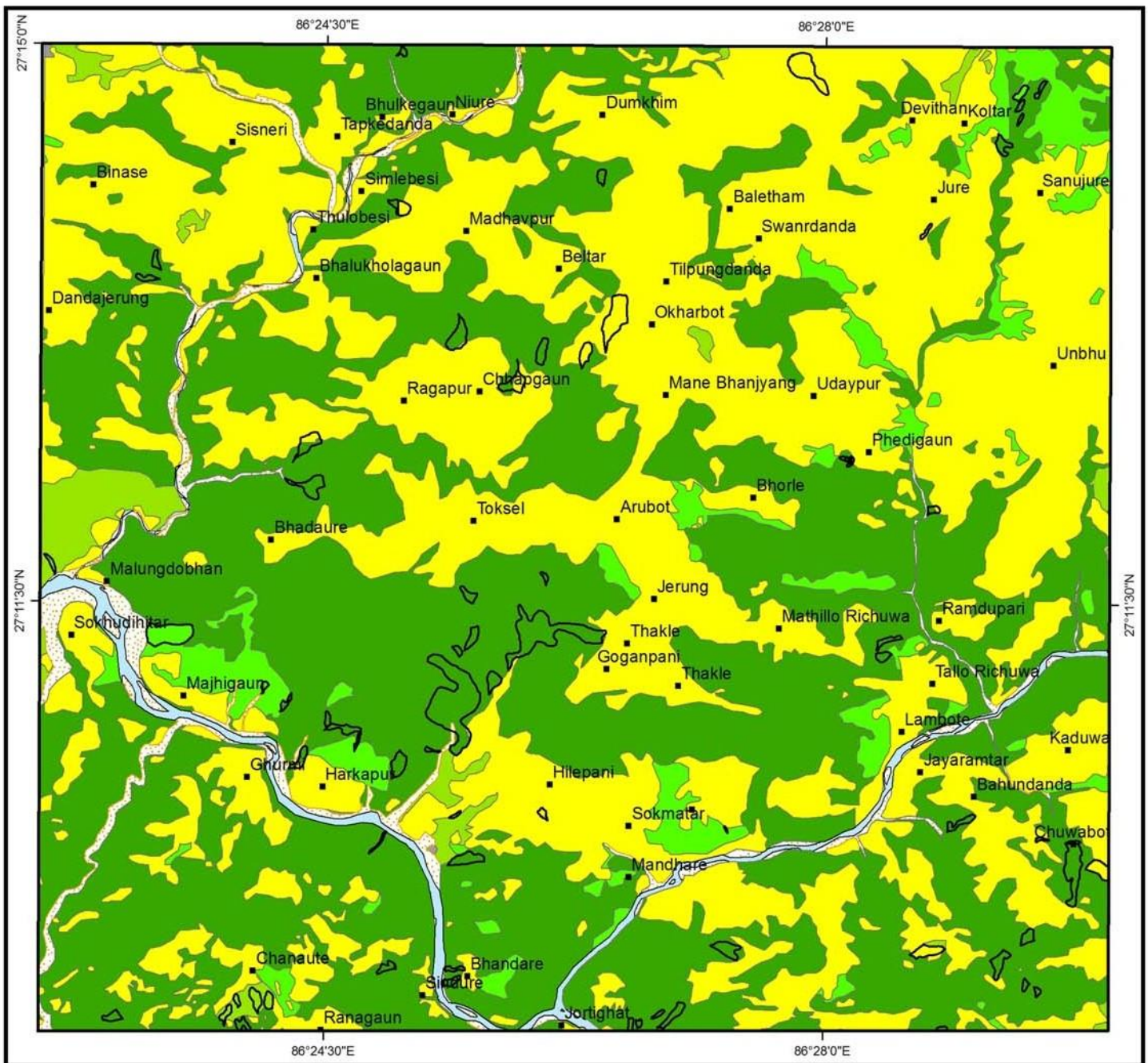


**Figure 4.7 Land cover map of the study area**

**Table 4.3 Percentage coverage of land cover classes and occurrence of landslides in each class**

Land cover classes	Percentage covered	Percentage of landslide occurrence
Cultivated and built-up	45.44	18.98
Forest	45.62	70.33
Grass	4.17	6.73
Bush	1.62	3.65
Sandy area	2.00	0.31
Water body	1.14	0.00
Barren	0.02	0.00

### Slope Aspect

The direction in which the slope faces is the slope aspect. Generally the area of slope, facing towards the sunlight and rainfall zone have a greater tendency of mass movement hazard in comparison with the slope in the rain shadow zone. In regions like ours where the south face gets more rain as well as sun is prone to weathering than the northern face. Consequently the south-facing slopes will have higher tendencies to fail. The aspect map (Figure 4.8) was derived from the Digital Elevation Model (DEM) obtained from the Triangulated Irregular Network (TIN). The TIN itself was generated from the elevation data of the digital map provided by the Survey Department. The slope aspect was grouped into nine classes viz. N, NE, E, SE, S, SW, W, NW and Flat.

The south- and west-facing slopes have more landslides in the area. The south faces of the slopes normally get more warmth in the daylight than the north-facing slopes. And during night they cool rapidly. This heating and cooling phenomenon helps in weathering (exfoliation) of the rocks on the south faces more than on the north faces. Also the south faces get more rainfall and this also plays a vital role in triggering instability. The Malung Khola flowing from the north to south lies in the western extremity of the study area and all its tributaries join it from the east to west. In this process they follow weak zones like beddings, foliations and joints. This may be the cause of high occurrence of landslides in the west-facing slopes. The percentages of landslide occurrence in the classes along with the area percentage they cover are depicted in Figure 4.9.



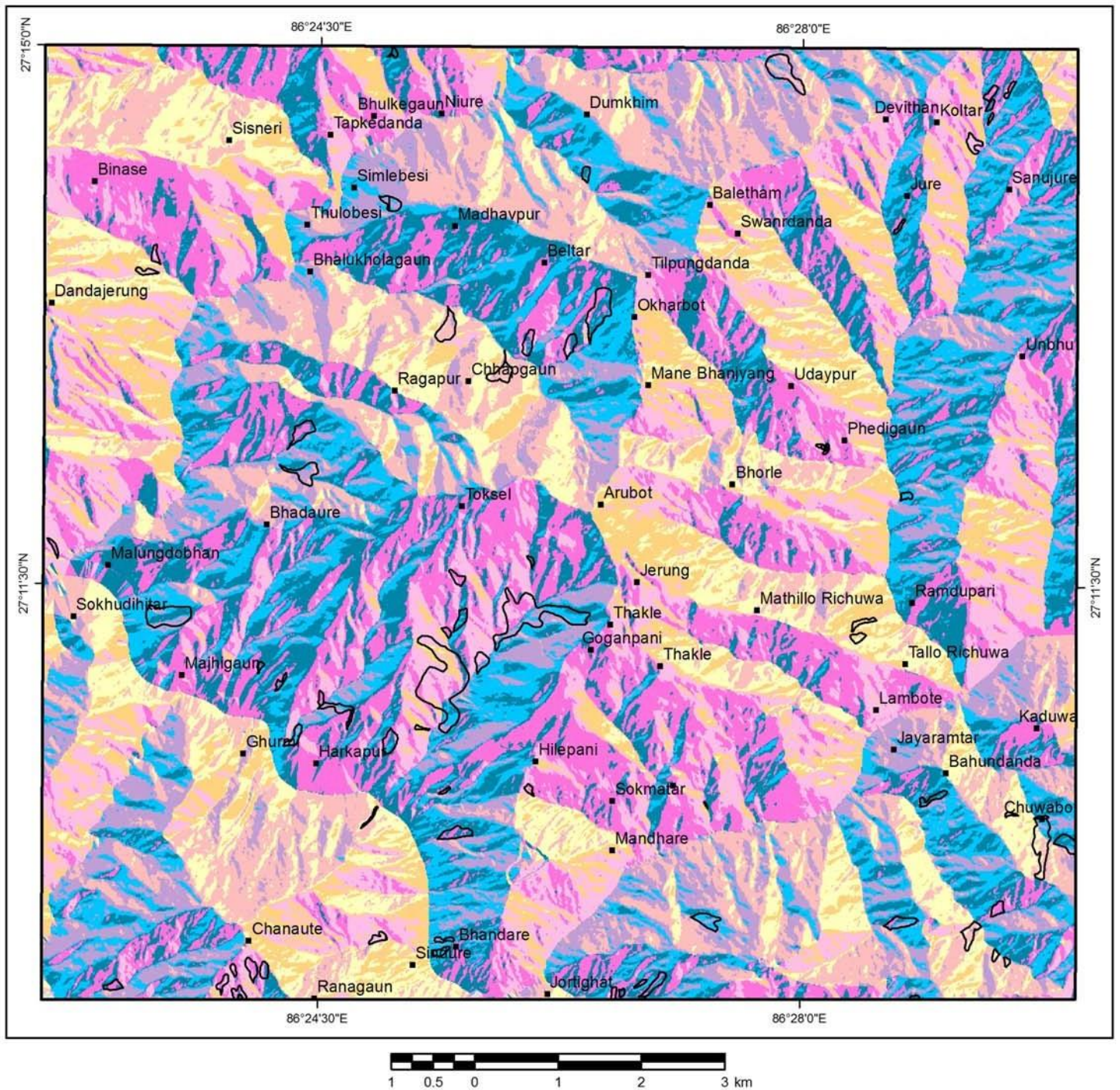
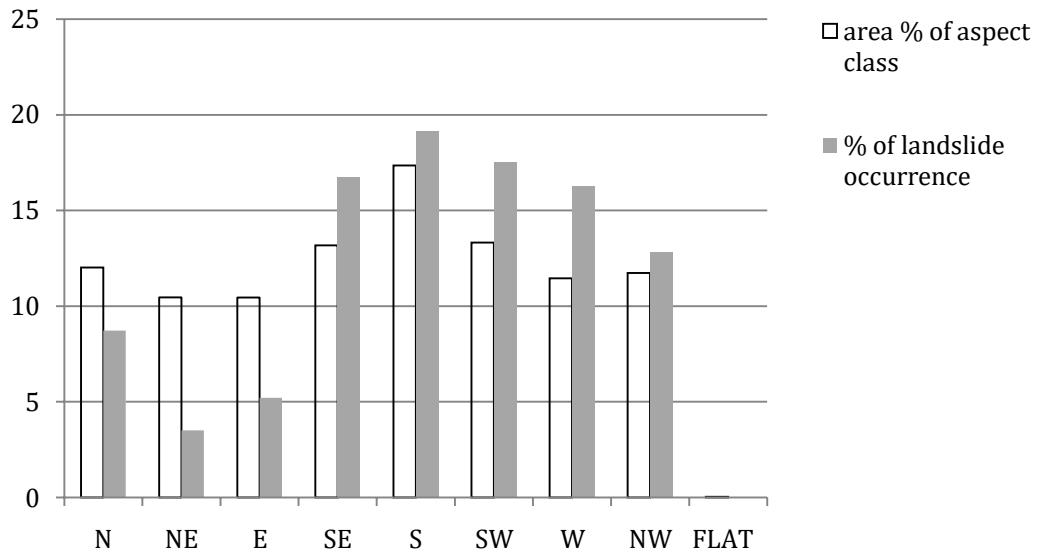


Figure 4.8 Slope aspect map of the study area





**Figure 4.9 Area percentage of aspect class and percentage of landslide occurrence**

### Slope Angle

Slope angle is considered as triggering factor for mass wasting because of the action of gravity. Generally steep slopes are prone to sliding than the gentle ones as friction angle of the material and earth's gravity come into play. The slope angle is also derived from the DEM. The slope angle of the present study area was categorised into five classes: less than 15°, 15–25°, 25–35°, 35–45° and more than 45° (Figure 4.10). The slope classes of 25–35° and 35–45° cover more area than other classes; 31.15% and 26.57% respectively. Very steep slopes (more than 45°) occupy 16.73% of the total area. The gentle slopes i.e. 15–25° cover 17.65% of the area and the slopes with less than 15° angle cover a minimum area of 7.91%. The mass movements are concentrated on the steep slopes compared to the gentle slopes. A majority of landslides have occurred in the slope classes of 25–35°, 35–45° and >45° (28.16%, 39.04% and 24.59% respectively). It is observed that the steeper slopes have more probability of mass wasting due to the earth's gravity.

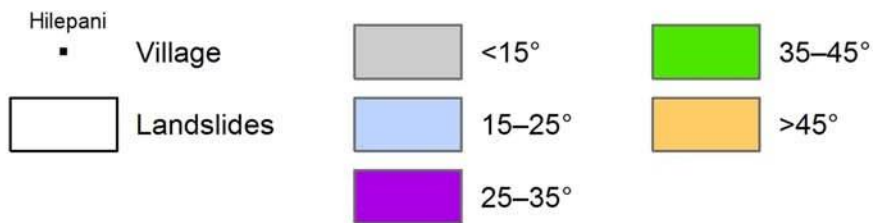
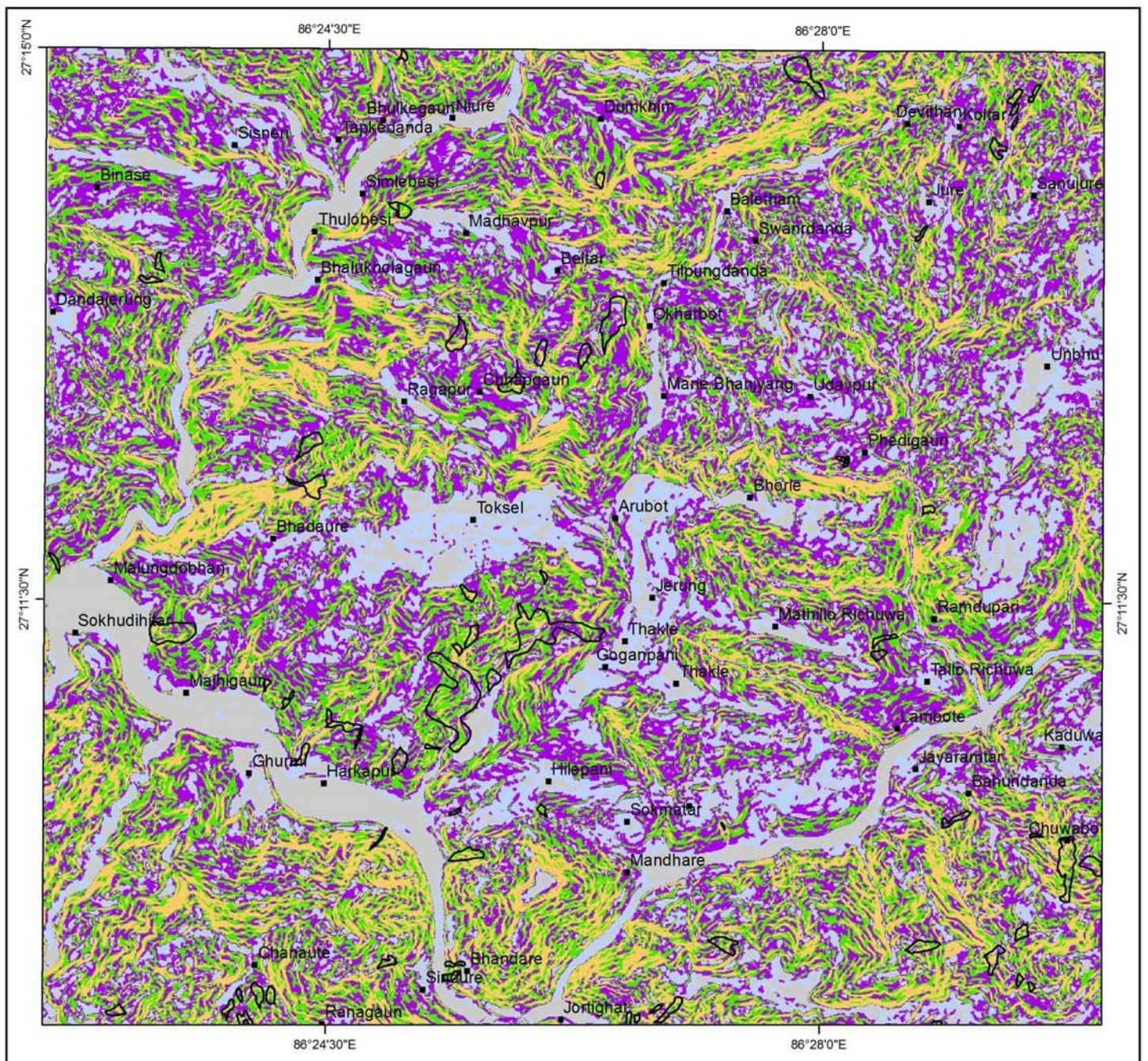


**Figure 4.10** Slope angle of the study area



## Altitude

Though altitude by itself is not a landslide triggering factor, there are some altitude ranges where the slope failures are frequent. Variation in elevation is high in the area with altitude ranging from less than 300 m to more than 1800 m. The altitude map, prepared from the DEM, has seven classes of altitude with an interval of 250 m: less than 500 m, 500–750 m, 750–1000 m, 1000–1250 m, 1250–1500 m, 1500–1750 m and more than 1750 m (Figure 4.11). It can be observed in Table 4.4 that most landslides occur on an altitude range of 750–1000 m. Normally, higher altitudes have higher rainfall and higher rate of weathering. It leads to slope instabilities on higher altitudes. In the study area a few landslides are observed above 1500 m because these classes cover lesser area. They lie in the ridges where there is a less tendency of slope failure. As the areal coverage of the altitude classes of 500–750 m, 750–1000 m and 1000–1250 m is more, more landslides occur there. The areas with altitude less than 500 m are the flat lands and consequently landslides are lacking.

**Table 4.4 Percentage coverage of altitude classes and occurrence of landslides in each class**

Altitude classes	Percentage covered	Percentage of landslide occurrence
<500 m	11.73	6.01
500–750 m	21.76	26.86
750–1000 m	23.18	38.73
1000–1250 m	20.31	14.78
1250–1500 m	14.29	12.68
1500–1750 m	7.75	0.94
>1750 m	0.97	0.00

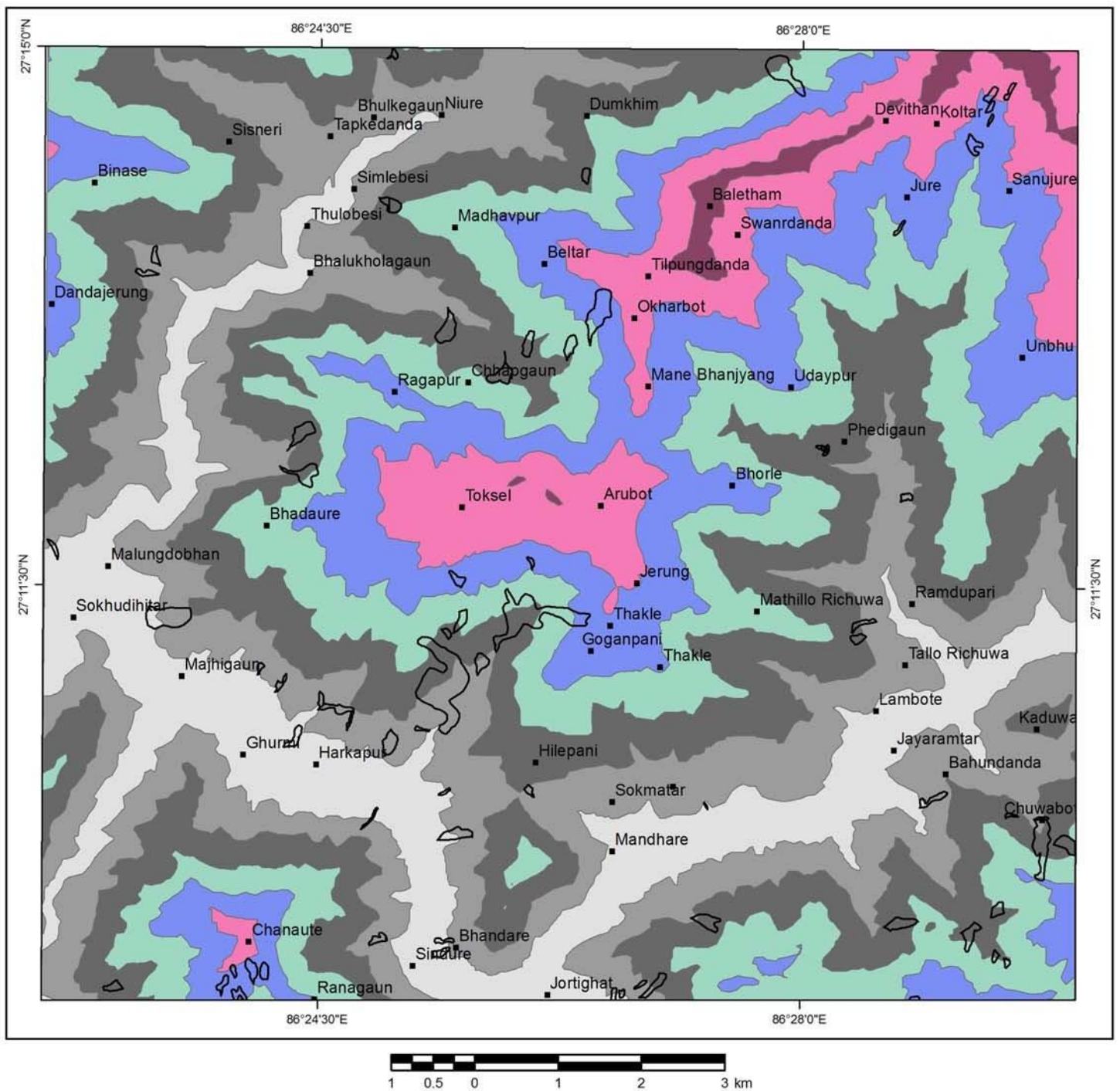


Figure 4.11 Altitude map of the study area

#### 4.2.9 Precipitation

Precipitation is another important factor that affects slope stability in areas like Nepal where maximum rainfall occurs in a short period of time. Rainfall data of more than 20 years from several rainfall stations is required for the preparation of rainfall distribution map. The present study area has only one rainfall station located almost at the centre of the study area at Manebhanjyang. Adjacent rainfall stations at Okhaldhunga, Gaighat and Hariharpurgadhi are far in comparison to the areal extent of the study area. As a result, the rainfall map produced using the data from these stations cannot be a real representation of the rainfall distribution in the study area. Nevertheless, a rainfall distribution map (Figure 4.12) was prepared with rainfall data of 30 years (1980-2009) from four rainfall stations (Manebhanjyang, Okhaldhunga, Gaighat and Hariharpurgadhi). This map was used as a causative factor map for susceptibility analysis. According to the map a majority of the existing landslides fall in the areas with lesser rainfall (Table 4.5), which could not be true. During bivariate analysis, error occurred as the resulting landslide susceptibility index map showed strong effect of the rainfall distribution. The reason behind this is the unreal representation of rainfall distribution owing to the lack of rainfall data around the study area. Hence the rainfall was not considered and susceptibility analysis was carried out with only above-mentioned 8 causative factors.

*Table 4.5 Percentage coverage of rainfall classes and occurrence of landslides in each class*

Average rainfall classes	Percentage covered	Percentage of landslide occurrence
<1100 mm/yr	10.29	10.43
1100–1200 mm/yr	60.89	78.18
1200–1300 mm/yr	24.18	3.94
>1300 mm/yr	4.64	7.45

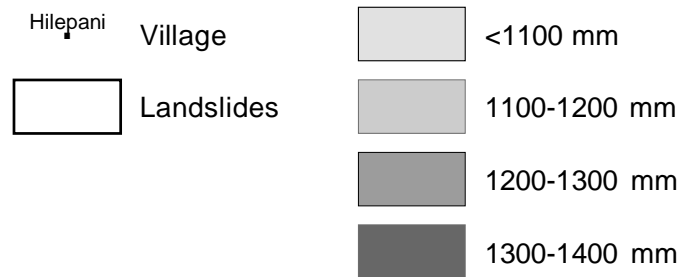
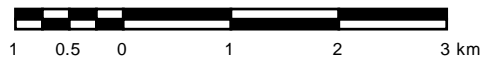
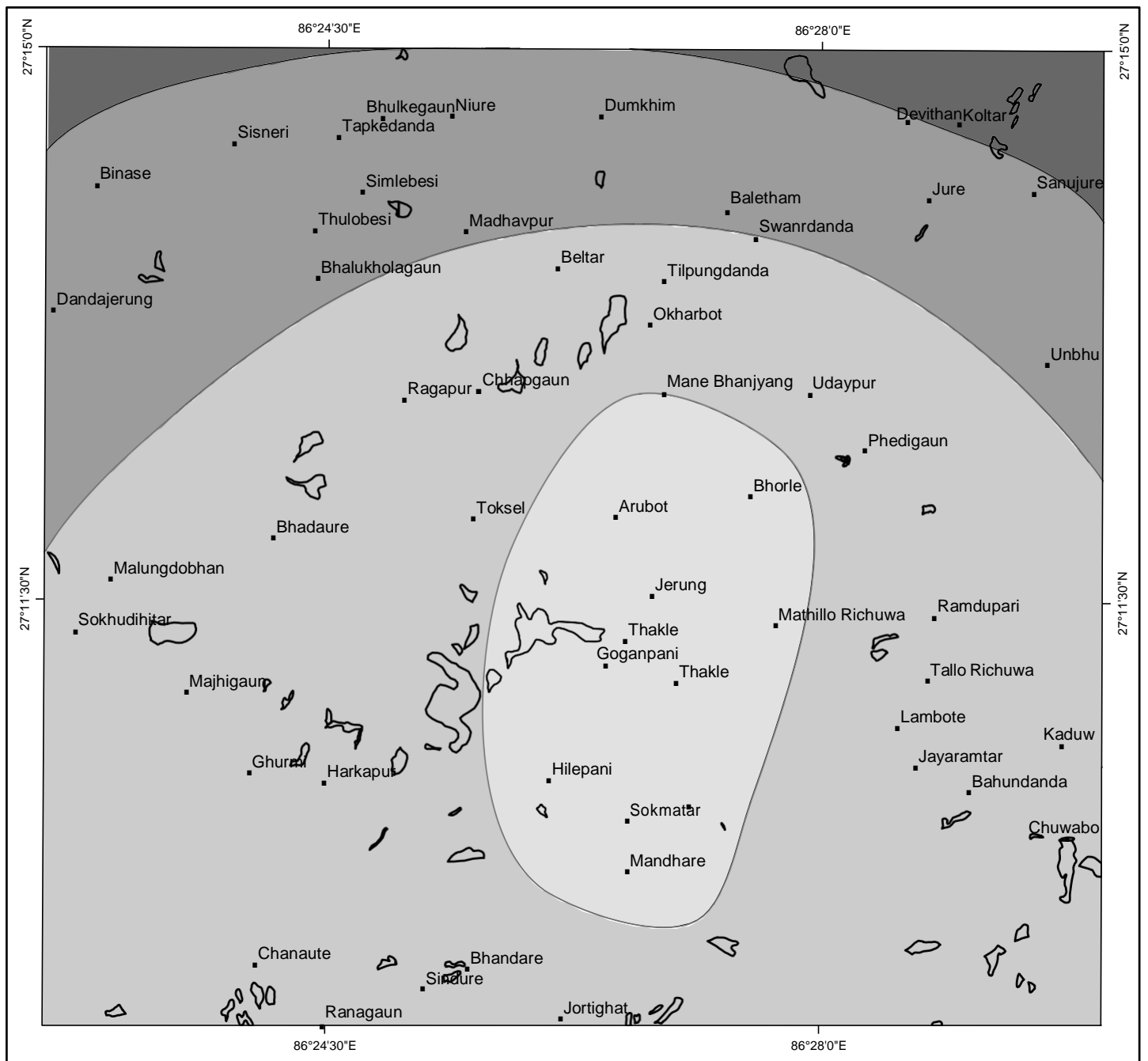


**Figure 4.12 Average annual rainfall distribution**

## CHAPTER FIVE

### LANDSLIDE SUSCEPTIBILITY MAPPING APPLYING HEURISTIC AND BIVARIATE METHODS

Different GIS methods for slope instability modelling are employed by various researchers all around the world. A general description on various methods of the landslide susceptibility analysis is presented below.

#### Landslide Susceptibility Analysis Methods

The methods for susceptibility analysis can be broadly divided into a) qualitative or quantitative and b) direct or indirect.

Qualitative methods use descriptive or qualitative terms to allocate susceptibility zones whereas quantitative methods give numerical estimates for depicting probability for landslide occurrence.

Direct methods study the existing landslides and delineate susceptibility area using specific knowledge of areas of potential instability whereas indirect methods use relative contribution of various causative factors of landslide to estimate the susceptible areas.

Many approaches used in the susceptibility mapping can be grouped in five categories as shown by Van Westen et al., (1997), in Table 5.1.

*Table 5.1 Characteristics of landslide susceptibility methods (Van Westen et. al. 1997)*

	Direct	Indirect	Qualitative	Quantitative
Geomorphological mapping	√		√	
Heuristic (index based)		√	√	
Analysis of inventories		√		√
Statistical modeling		√		√
Process based (deterministic)		√		√

The geomorphological mapping technique employs information of existing landslide and knowledge of the area to identify potential areas of instability.

Heuristic method is subjective, indirect and qualitative method which requires prior knowledge of the landslides and their processes in the area. The investigator or an expert assigns weights to causative factors of landslides and then these maps are combined to give a susceptibility index map. It uses the factor maps rated by an expert based on his/her field knowledge of the area.

Analysis of inventory method utilise the map of existing landslides to predict landslide prone areas. The analysis of this distribution can lead to the extrapolation to other areas of possible instabilities and classification into a final instability map (Guzzeti et. al., 1999).

Statistical tools or methods are used to determine the relationship between instability factors and existing landslides. This quantitative and purely statistical method can be divided as bivariate and multivariate methods.

In bivariate method, the factor maps are assigned weight according to the relationship of landslide inventory map with each of them. Each factor map is overlaid with landslide map to find relation between each factor and its classes. Weights are assigned to each class using different statistical rules. Then the weighted factor maps are combined to give a susceptibility index map which is further classified into susceptibility zones. Different bivariate methods vary with each other only in the way the weights are produced using different statistical rules. Statistical index method of Van Westen (1997) is used in the present study.

In multivariate analysis, relative contribution of each factor for instability is determined by statistical analysis of causative factors.

Process based or deterministic models include assessment of susceptibility zones by considering physical laws controlling slope instability. The models calculate the stability of slope using parameters as normal stress, angle of friction, cohesion, pore-water pressure, seismic acceleration etc. This results in calculation of factor of safety based on which instability map is prepared.



## **Previous Works on Landslide Susceptibility Mapping in Nepal**

Few attempts have been made so far on hazard mitigation and to prepare maps depicting the hazard and/or risk associated with landslides in Nepal (Upreti and Dhital, 1996). Even though studies of other aspects of landslide were started in Nepal from the decade of sixty, it can be said that the landslide hazard mapping started much later. Wagner et al. (1988) developed a computer program for rock and debris slide hazard mapping and prepared rock and debris slide risk map of Nepal. Till date several researchers have worked with various analytical approaches for the landslide susceptibility mapping. Deoja et al., 1991; Thapa and Dhital, 2000; Koirala and Adhikary, 2007; Kayastha et al., 2010 used the heuristic approach. Statistical analysis methods are used by Sikrikar et al., 1998; Dhakal et al., 1999; Ghimire, 2001; Dangol and Ulak, 2002; Paudyal and Dhital, 2005; Dhital et al., 2005; Dahal et. al, 2008; Pantha et al., 2010; Poudyal et al., 2010; Kayastha et al., 2010 and deterministic techniques were used by Joshi et al., 2000; Acharya et al., 2006; Sharma and Shakya, 2008; Ray and De Smedt, 2009; Kayastha and De Smedt, 2009 for landslide susceptibility mapping.

### **Landslide Susceptibility Analysis in the Study Area**

Out of numerous methods of landslide susceptibility mapping, two were applied in the present study: heuristic and bivariate method. As mentioned earlier, eight causative factors were considered for the study. These factors were presented as factor maps which were taken into account for susceptibility analysis. The two methods used to produce two different landslide susceptibility maps are described in this chapter together with the results they produced.

#### **Heuristic Method for Landslide Susceptibility Mapping**

Heuristic method is an approach in which a researcher assigns weight based on expert opinion or personal experience. Out of different methods of heuristic methods index-based method was used in the present study.

### ***Methodology for Index-based Analysis Method***

The index-based analysis method was first proposed by Deoja et al., 1991. In this method the causative factors of the slope instability of the study area are selected and each factor is considered a parameter map. Each parameter map is also divided into number of classes depending on their influence on the slope instability. Then the relative importance of parameter map for slope instability is evaluated according to the expert's knowledge. According to the comparison of different parameter maps weight values are assigned to each map and rating values are also assigned to each class of every parameter map.

The integration of the various factors in a single landslide susceptibility index (LSI) is accomplished by a procedure based on the weighted linear sum

$$LSI = \sum_{j=1}^n w_j x_{ij}$$

where

LSI: landslide susceptibility index

$w_j$ : weight value of parameter j

$x_{ij}$ : rating value of class i of parameter j

n: number of parameters

### ***Results and Discussions***

The weight given to each parameter together with the ratings assigned to each of its classes must reflect the relative importance it has on the slope stability. In the present study, the total weight of all eight factors was considered to be 100. The different factors were then assigned weight relative to other factors and their effect on slope instability by the supervisor of the study. Accordingly the classes of each factors were also given rating varying from 0 to 10, where 0 meaning no effect and 10, the most on landslide occurrence. In the study area slope angle, drainage distance, geology and land cover were considered the most influencing factors for slope instability hence were assigned weight ranging from 18 to 14. In contrast, distance from faults-fold axis was given less weight as it was considered

to have relatively less effect on landslide occurrence. The ratings to each class were assigned by considering their relative effect on the cause of landslides. For example, in slope angle parameter, maximum ratings were assigned to slope classes of 35–45° and more than 45° whereas minimum rating was assigned to very flat slopes (Figure 5.1). Similarly the ratings assigned to the classes of distance from drainage, and soil-rock type is graphically represented in Figure 5.2 and 5.3 respectively as examples. The weight and ratings assigned to the factors and classes is tabulated in Table 5.2.

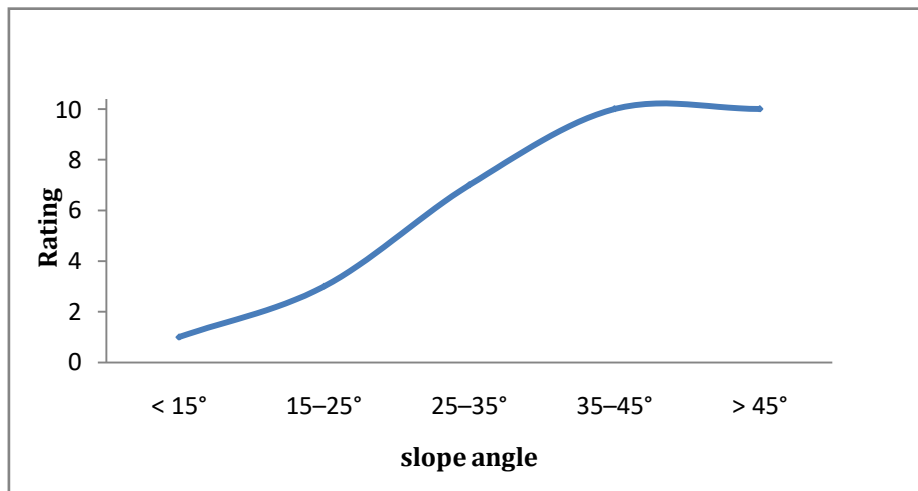


*Figure 5.1 Distribution of ratings for slope angle classes*

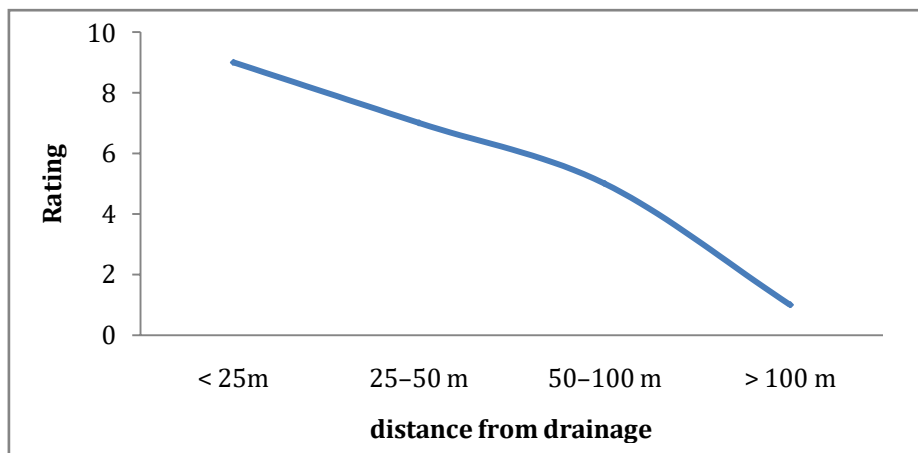


*Figure 5.2 Distribution of ratings for distance from drainage classes*

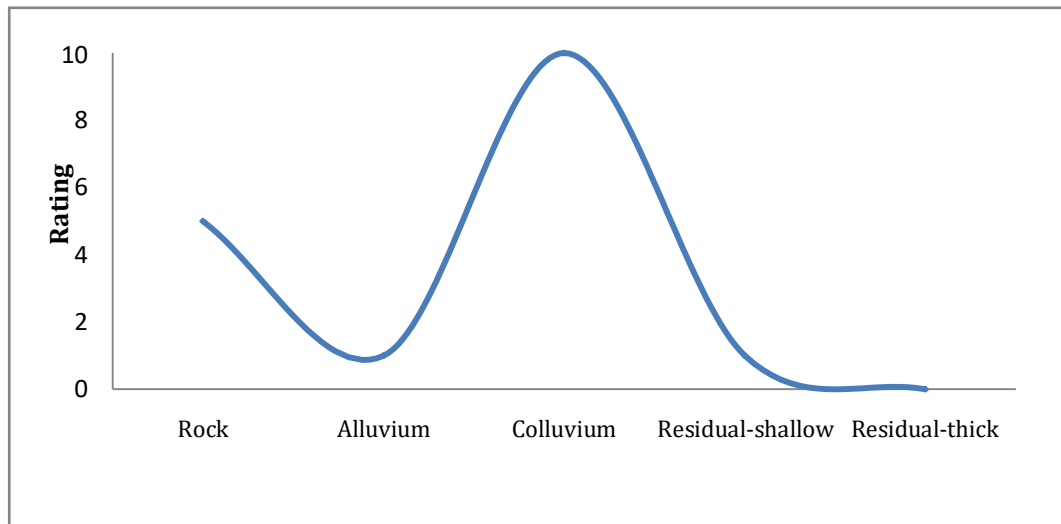


**Figure 5.3 Distribution of ratings for rock or soil map**

**Table 5.2 Weight and ratings assigned to parameters**

<b>Causative Factors</b>	<b>Rating (<math>x_{ij}</math>)</b>	<b>Weight (<math>w_j</math>)</b>	<b>Final weight (<math>w_j * x_{ij}</math>)</b>
<b><i>Geology</i></b>			
Harkapur Formation	5	14	70
Madhavpur Slates	2		28
Haleshi Dolomite	10		140
Para Khola Formation	1		14
Higher Himalayan Crystalline	3		42
<b><i>Distance from faults-folds</i></b>			
<50 m	9	8	72
50-100 m	5		40
>100 m	1		8
<b><i>Distance from drainage</i></b>			
< 25m	9	14	126
25-50 m	7		98
50-100 m	5		70
> 100 m	1		14
<b><i>Rock and soil Type</i></b>			
Rock	5	10	50
Alluvium	1		10
Colluvium	10		100
Residual-shallow	1		10
Residual-thick	0		0

**Table 5.2 Weight and ratings assigned to parameters (contd.)**

<b>CausativeFactors</b>	<b>Rating (<math>x_{ij}</math>)</b>	<b>Weight (<math>w_j</math>)</b>	<b>Final weight (<math>w_j * x_{ij}</math>)</b>
<b><i>Land cover</i></b>			
Cultivated and built-up	2	14	28
Forest	7		98
Grass	7		98
Bush	10		140
Sandy area	1		14
Water body	0		0
Barren	0		0
<b><i>Slope Aspect</i></b>			
N	3	12	36
NE	1		12
E	2		24
SE	5		60
S	5		60
SW	5		60
W	6		72
NW	4		48
FLAT	1		12
<b><i>Slope Angle</i></b>			
0-15°	1	18	18
15-25°	3		54
25-35°	7		126
35-45°	10		180
>45°	10		180
<b><i>Altitude</i></b>			
<500 m	3	10	30
500-750 m	7		70
750-1000 m	9		90
1000-1250 m	4		40
1250-1500 m	5		50
1500-1750 m	1		10
>1750 m	0		0

The landslide susceptibility index was calculated by summation of all score values obtained by multiplying weight and rating assigned to factors and their classes. This was done by using Image Calculator tool in GIS application. The result was Landslide Susceptibility Index (LSI) map (Figure 5.4), where the LSI values ranges from 108 to 858.

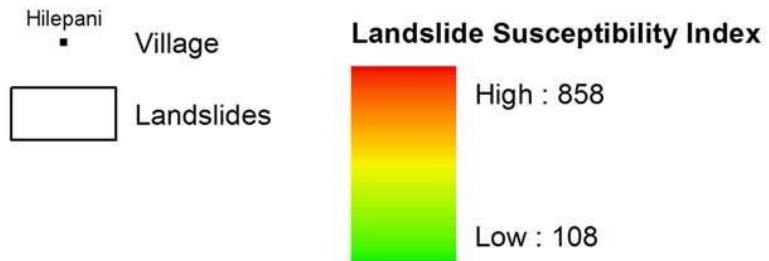
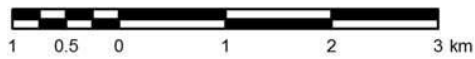
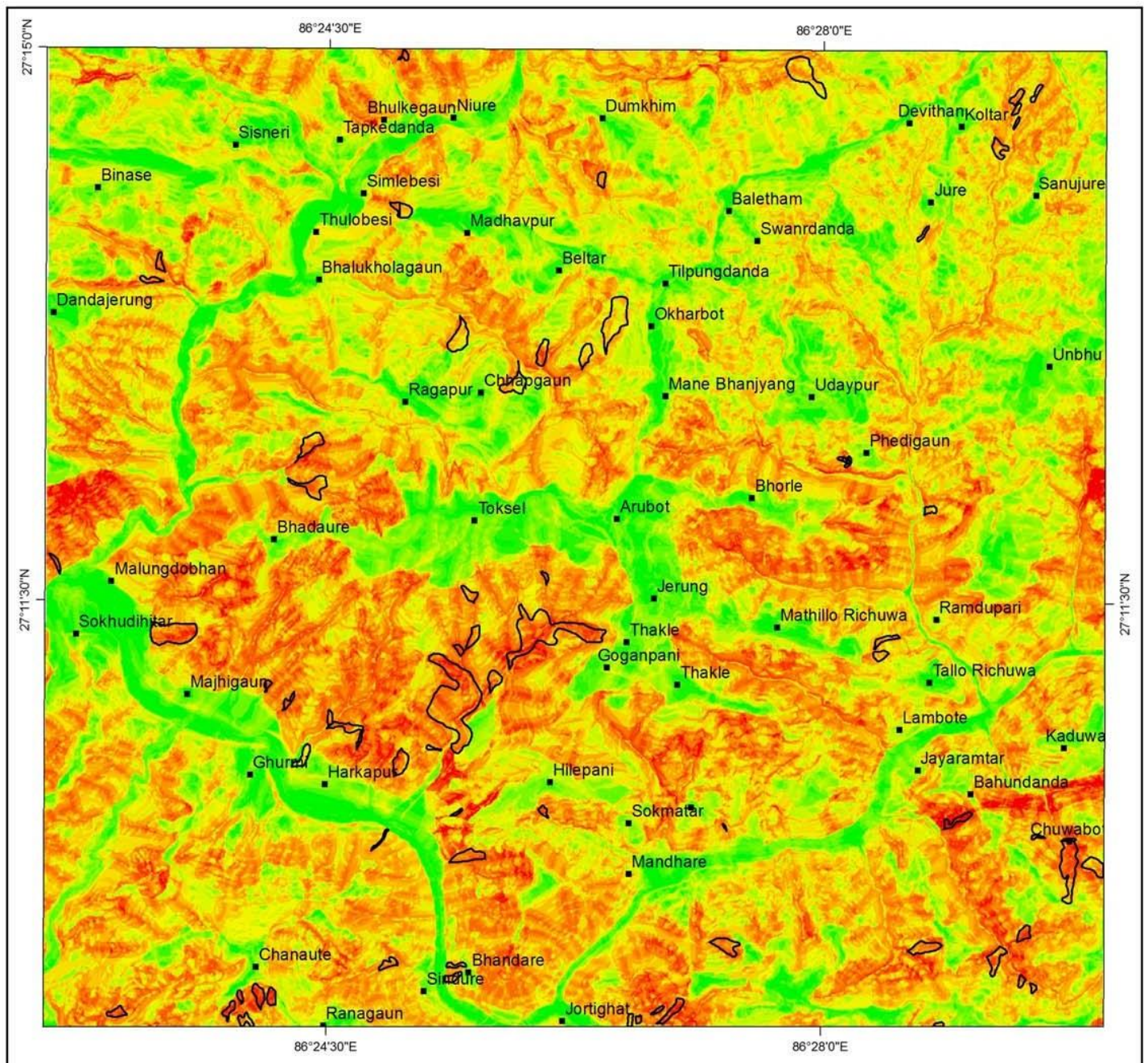


*Figure 5.4 Landslide Susceptibility Index obtained with index-based method*



But as the LSI map cannot be used properly to assess the hazards, reclassification of the LSI values into different susceptibility classes is necessary. This procedure known as landslide susceptibility zonation can be done in many ways. But there is no statistical rule for the purpose and many researchers have their own methods of classifying the index values into susceptibility zones. Some use classifying methods provided in GIS applications which base the classification into equal intervals, natural breaks or quartile and standard deviation methods. But most researchers use their own expert opinion to manually classify the class boundaries.

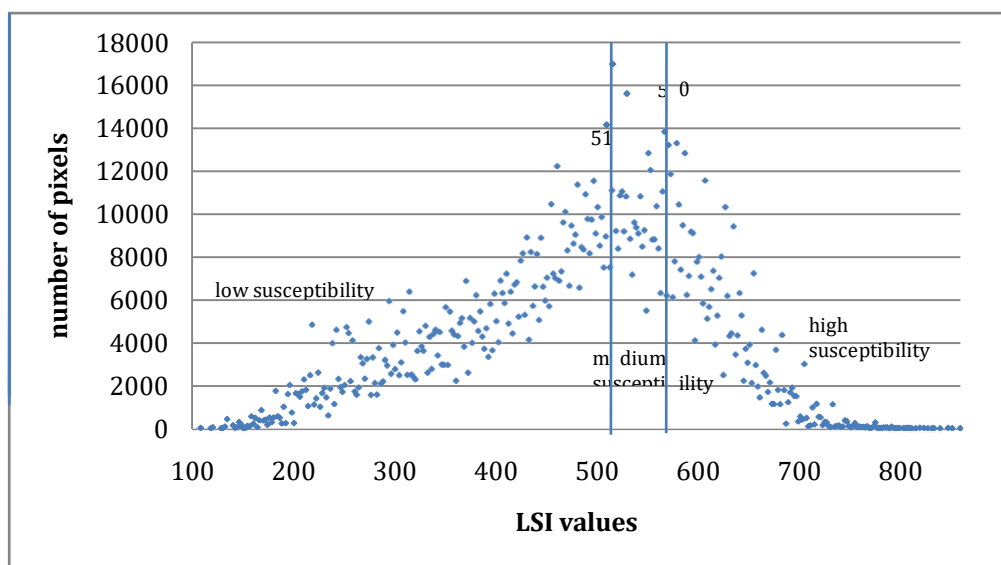


**Figure 5.5 Classification of LSI values based on natural break method**

In the present study, the classification is done with natural break method. For this purpose the number of pixels in each index score was plotted (Figure 5.5) and classes were defined according to conspicuous breaks in the resulting chart. The LSI values below 516 was considered as low susceptible whereas above 570 was considered as high. The values in between the two were considered medium susceptible to landslide. The resulting map of landslide susceptibility zonation is shown in Figure 5.6 along with existing landslides.

According to the map 56.31% (79.583 km<sup>2</sup>) area lies in the low susceptibility zone whereas the area under medium and high susceptibility zones are 18.92% (26.743 km<sup>2</sup>) and 24.77% (35.001 km<sup>2</sup>) respectively. Table 5.3 depicts the areal



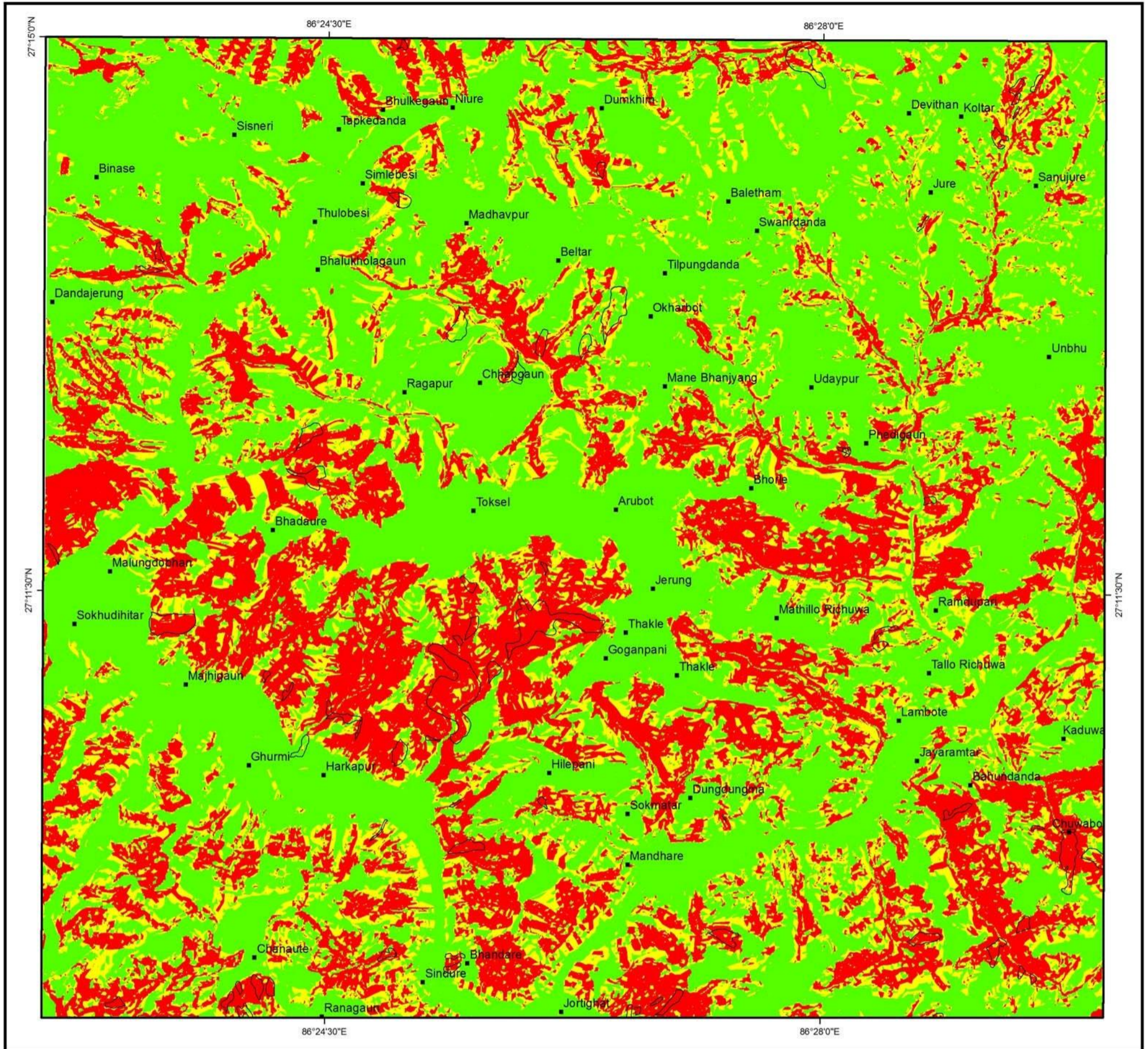


Figure 5.6 Landslide Susceptibility Zonation map using index-based method



relationship of the susceptibility zones along with percentage of landslide occurrence in the zones.

**Table 5.3 Distribution of landslide susceptibility zones and landslide occurrence**

Susceptibility zones	Area		Landslide area	
	km <sup>2</sup>	percent	km <sup>2</sup>	percent
Low	79.583	56.31	0.257	12.43
Medium	26.743	18.92	0.367	17.75
High	35.001	24.77	1.445	69.82
<b>Total</b>	<b>141.327</b>	<b>100.00</b>	<b>2.069</b>	<b>100.00</b>

According to the susceptibility map (Figure 5.6) the high susceptible areas for landslides are the Bhadare Khola section northeast of Harkapur, Majhigau, Chuwabot, Phedigau, Koltar, Bhulkegau, Bhalu Khola, and areas around Sokmatar. These may be due to the fragile lithology and gulley erosion of the rivers. Mostly the river sections are more hazardous due to the steep slope and the action of river. The Ghurmi, Hilepani, Arubot, Manebhanjyang, Udaypur, Toksel and Unbhu villages are in the low susceptibility zones. Generally areas near streams with steep slope and fragile lithology with bush as land cover are the most hazardous region for landslide occurrence. Based on lithology parameter it is observed that the Harkapur Formation has the highest susceptibility for landslide occurrences.

### **Bivariate Method for Landslide Susceptibility Mapping**

Bivariate analysis method uses the landslide densities within each parameter map and its classes to derive weight values for those classes. It is based on the assumption that causative factors of landslides can be quantified by calculating landslide densities of each class. These weighted parameter maps are then combined to produce a landslide susceptibility map. The result of bivariate analysis methods depends on the selection of parameters or causative factors for slope instability. This method is termed bivariate as it compares a dependent variable (landslide inventory map in this case) to each factor (independent variables) separately and the importance of each factor is determined

independently of other factors. There are various bivariate analysis methods where the difference is the technique used to derive the weight of the factor classes. The present study is based on the Statistical Index method.

***Methodology for Statistical-Index method***

This bivariate method was first introduced by Van Westen (1997) for landslide susceptibility analysis.

In the statistical index method, a weight value for a parameter class, such as a certain lithological unit or a certain slope class is defined as the natural logarithm of the landslide density in the class divided by the landslide density in the entire map. This method is based upon the following formula (Van Westen, 1997):

$$w_{ij} = \ln \frac{f_{ij}}{f} = \ln \left( \frac{A^*_{ij}}{A_{ij}} \times \frac{A}{A^*} \right) = \ln \left( \frac{A^*_{ij}}{A^*} \times \frac{A}{A_{ij}} \right)$$

where

$w_{ij}$ = weight given to class i of parameter j

$f_{ij}$ = landslide density within class i of parameter j

$f$  = landslide density within entire map

$A^*_{ij}$ = area of landslide in class i of parameter j

$A_{ij}$ = area of a class i of parameter j

$A^*$ = total area of landslides in entire map

$A$ = total area of entire map

Different causative factor maps are developed using the weights derived from above relation in the GIS application. The resultant landslide susceptibility index map is prepared by overlaying the weighted parameter maps in the GIS application. The process can be represented by following equation:

$$LSI = \sum_{j=1}^n w_{ij}$$

where

LSI= landslide susceptibility index

$w_{ij}$ = weight of class i of parameter j

n= number of parameters

### **Results and Discussions**

The weights of each class of all 8 parameters derived using the above relation is shown in [Table 5.4](#).

**Table 5.4 Derivation of weight values of parameter classes by bivariate method**

<b>CausativeFactors</b>	<b><math>A_{ij}</math></b>	<b><math>A_{ij}/A \%</math> (<math>A=141.237 \text{ km}^2</math>)</b>	<b><math>A^*_{ij}</math></b>	<b><math>A^*_{ij}/A^* \%</math> (<math>A^*=2.069 \text{ km}^2</math>)</b>	<b><math>w_{ij}</math></b>
<b><i>Geology</i></b>					
Harkapur Formation	44.80	31.70	0.97	46.94	0.39
Madhavpur Slates	57.62	40.77	0.57	27.37	-0.40
Haleshi Dolomite	0.28	0.19	0.02	0.81	1.42
Para Khola Formation	4.54	3.21	0.01	0.34	-2.24
Higher Himalayan Crystallines	34.09	24.12	0.51	24.54	0.02
<b><i>Distance from faults-folds</i></b>					
<50 m	4.31	3.05	0.05	2.59	-0.17
50-100 m	4.59	3.25	0.05	2.48	-0.27
>100 m	132.43	93.70	1.96	94.93	0.01
<b><i>Distance from drainage</i></b>					
< 25 m	31.35	22.18	0.81	39.05	0.57
25-50 m	24.38	17.25	0.48	23.29	0.30
50-100 m	45.35	32.09	0.58	28.15	-0.13
> 100 m	40.25	28.48	0.20	9.51	-1.10
<b><i>Rock and soil type</i></b>					
Rock	55.43	39.22	0.72	34.88	-0.12
Alluvium	10.92	7.72	0.02	0.82	-2.24
Colluvium	48.12	34.05	1.32	63.56	0.62
Residual-shallow	25.57	18.09	0.02	0.74	-3.20
Residual-thick	1.29	0.91	0.00	0.01	-4.51

**Table 5.4 Derivation of weight values of parameter classes by bivariate method (contd.)**

<b>CausativeFactors</b>	<b>A<sub>ij</sub></b>	<b>A<sub>ij</sub>/A % (A=141.237 km<sup>2</sup>)</b>	<b>A*<sub>ij</sub></b>	<b>A*<sub>ij</sub>/A* % (A*=2.069 km<sup>2</sup>)</b>	<b>w<sub>ij</sub></b>
<b><i>Land cover</i></b>					
Cultivated and built-up	64.22	45.44	0.39	18.98	-0.87
Forest	64.47	45.62	1.46	70.33	0.43
Grass	5.89	4.17	0.14	6.73	0.48
Bush	2.29	1.62	0.08	3.65	0.81
Sandy area	2.82	2.00	0.01	0.31	-1.86
Water body	1.61	1.14	0.00	0.01	-4.74
Barren	0.03	0.02	0.00	0.01	-0.64
<b><i>Slope Aspect</i></b>					
N	16.98	12.01	0.18	8.72	-0.32
NE	14.79	10.46	0.07	3.50	-1.10
E	14.77	10.45	0.11	5.20	-0.70
SE	18.63	13.18	0.35	16.77	0.24
S	24.53	17.35	0.40	19.15	0.10
SW	18.83	13.32	0.36	17.53	0.27
W	16.19	11.45	0.34	16.30	0.35
NW	16.58	11.73	0.27	12.82	0.09
FLAT	0.04	0.03	0.00	0.01	-1.18
<b><i>Slope Angle</i></b>					
0–15°	11.18	7.91	0.03	1.21	-1.87
15–25°	24.94	17.65	0.14	7.00	-0.92
25–35°	44.02	31.15	0.58	28.16	-0.10
35–45°	37.54	26.57	0.81	39.04	0.38
>45°	23.65	16.73	0.51	24.59	0.38
<b><i>Altitude</i></b>					
<500 m	16.58	11.73	0.12	6.01	-0.67
500–750 m	30.76	21.76	0.56	26.86	0.21
750–1000 m	32.76	23.18	0.80	38.73	0.51
1000–1250 m	28.71	20.31	0.31	14.78	-0.32
1250–1500 m	20.20	14.29	0.26	12.68	-0.12
1500–1750 m	10.95	7.75	0.02	0.94	-2.11
>1750 m	1.37	0.97	0.00	0.01	-4.58

This method calculates  $w_{ij}$  to classes which have landslide occurrence but due to the natural logarithm, it cannot determine the weight for classes where there is no landslide occurrence. Some researchers assign weight value of 0 to those parameter classes but it will mean that the particular class will have no correlation to the landslide occurrence which may not be the real case. So in the present study the parameter class with no landslide occurrence is given a minimal value i.e. 0.01 to acknowledge their effect (though minimal) to the slope stability.

By combining all the weights of the parameter classes using the overlay function in GIS application, a LSI map (Figure 5.7) was prepared.

The landslide susceptibility index of the map varied from -14.42 to 3.81. As mentioned earlier the LSI map should be classified into susceptibility zones to facilitate assessment of hazards, it was classified according to natural break method using the scatter plot of weight value and the number of pixels (Figure 5.8). The LSI values less than -0.61 was classified as low susceptibility zone, values between -0.61 and 0.4 were considered medium susceptibility zone and values more than 0.4 were considered highly susceptible.

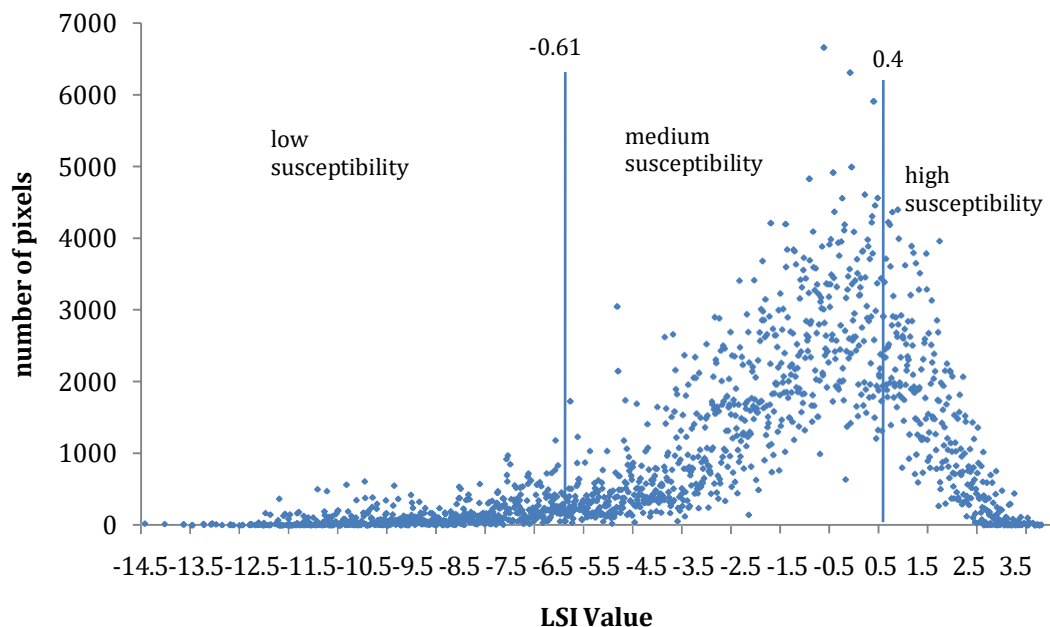


**Figure 5.8 Classification of LSI values based on natural break method**

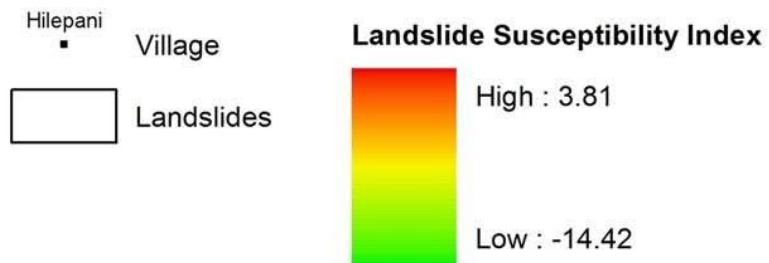
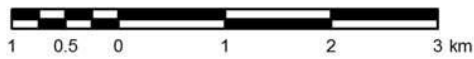
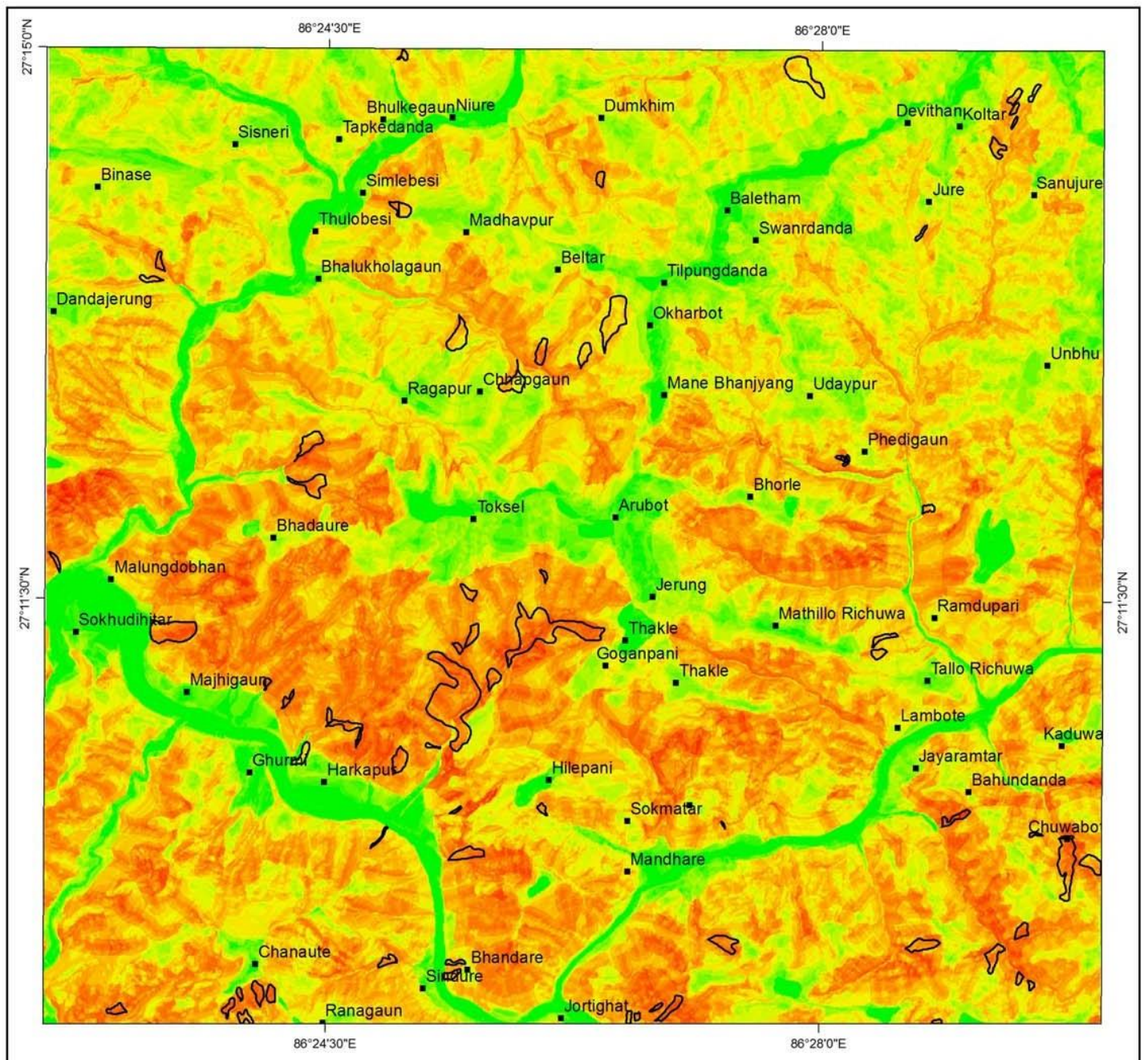


**Figure 5.7 Landslide Susceptibility Index obtained with statistical-index method**



The landslide susceptibility zonation map (Figure 5.9) was prepared using the above classification. According to the map, 50.89% (71.919 km<sup>2</sup>) area lies in the low susceptibility zone, 21.08% (29.797 km<sup>2</sup>) in medium susceptibility zone and 28.03% (39.611 km<sup>2</sup>) in high susceptibility zone. The areal relationship of the susceptibility zones along with their landslide occurrence is tabulated in Table 5.5.

**Table 5.5 Distribution of landslide susceptibility zones and landslide occurrence in them**

Susceptibility zones	Area		Landslide area	
	km <sup>2</sup>	percent	km <sup>2</sup>	percent
Low	71.919	50.89	0.179	8.66
Medium	29.797	21.08	0.359	17.37
High	39.611	28.03	1.531	73.98
<b>Total</b>	<b>141.327</b>	<b>100.00</b>	<b>2.069</b>	<b>100.00</b>

In the landslide susceptibility map prepared by bivariate analysis (Figure 5.9), flat areas like river valleys, terraces and ridges in the vicinity of Sokhuditar, Ghurmi, Harkapur, Hilepani, Jortighat, Tallo Richwa, Mathillo Richuwa, Arubot, Unbhu, Udaypur, Manebhanjyang, Devithan and Sisneri lie in the low landslide susceptible zone whereas villages like Dhumkhim, Madhavpur, Ragapur and Malungdobhan lie in the medium susceptibility zones. The steep slopes on sides of the river and streams lie in the high susceptible zones. The areas northeast of Harkapur, north and south of Hilepani, Bahundada, Chuwabot, Phedigau and Majhigau lie in the high susceptible areas for landslides. Most of the west study area lies in the high susceptible region which is due to a large number of landslides on the fragile and crushed lithology of the Harkapur Formation. The areas in high susceptibility zones but presently devoid of any failures indicate potential landslide areas.



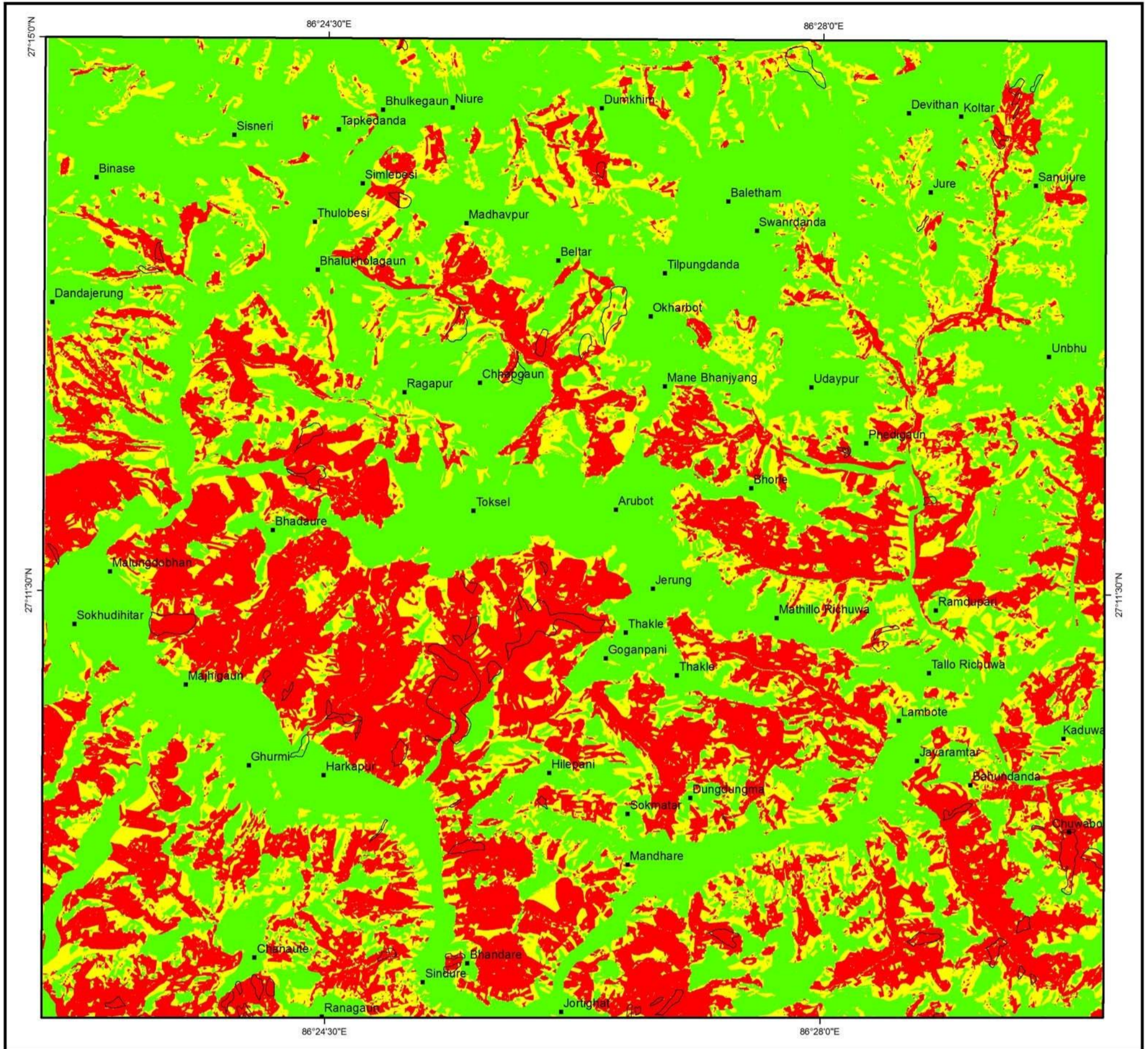


Figure 5.9 Landslide Susceptibility Zonation map using statistical-index method



## Comparison of landslide Susceptibility Maps

The landslide susceptibility zonation maps produced employing two different methods viz. index-based approach of heuristic method and statistical-index approach of bivariate method are validated and compared based on landslide density, success rate and percentage of agreed area between them. This is carried out to find the success of the analysis and the degree of agreement between the susceptibility maps derived from two different analysis methods.

### Comparison Based on Landslide Density

Landslide density is the ratio of area of existing landslide to the area of each landslide susceptibility class. In the present study, it is calculated on the basis of number of pixels. In an ideal landslide susceptibility map, the high susceptibility zone should have the highest landslide density and there should be a decreasing trend of the density values successively from medium to low susceptibility zones. The landslide densities of the susceptibility classes of both the Landslide Susceptibility Zonation (LSZ) maps are calculated and tabulated in the [Table 5.6](#).

*Table 5.6 Comparison of landslide densities of landslide susceptibility zones*

Susceptibility zones	Heuristic method			Bivariate method		
	area (km <sup>2</sup> )	landslides (km <sup>2</sup> )	landslide density	area (km <sup>2</sup> )	landslides (km <sup>2</sup> )	landslide density
Low	79.583	0.257	0.0032	71.919	0.179	0.0025
Medium	26.743	0.367	0.0137	29.797	0.359	0.0121
High	35.001	1.445	0.0413	39.611	1.531	0.0386

From the above table it is evident that landslide densities gradually increase from low susceptibility zones to high susceptibility zones in both cases. Landslide density of 0.0413 in high susceptibility zone in LSZ of heuristic method is remarkable higher than that of low and medium susceptibility zones. Similarly in LSZ of bivariate analysis, landslide density of 0.0386 in high susceptibility zone is quite higher than other two zones. This reflects the validity of both

landslide susceptibility maps. The densities are very similar in low and medium zones in both the maps whereas the LSZ of heuristic method showed a wee higher density in the high susceptibility zone.

### Comparison Based on Success Rate Curve

Percentage of landslide occurrence in any susceptible zone is termed success rate. This is also a way to validate a susceptibility map. The suitability of a map can be judged by the fact that more percentage of landslides must occur in high susceptibility zone as compared to other zones (Sarkar, 2008). The cumulative percentage of landslide occurrences in the susceptibility zones ordered from high to low are plotted against the cumulative percentage of area of the susceptibility zones. The resulting curve is called success rate curve. The area under the curve evaluates the accuracy of the analysis method qualitatively. The success rate curve for both the LSZ maps are shown in a single graph (Figure 5.10) for the ease of comparison between the two maps.

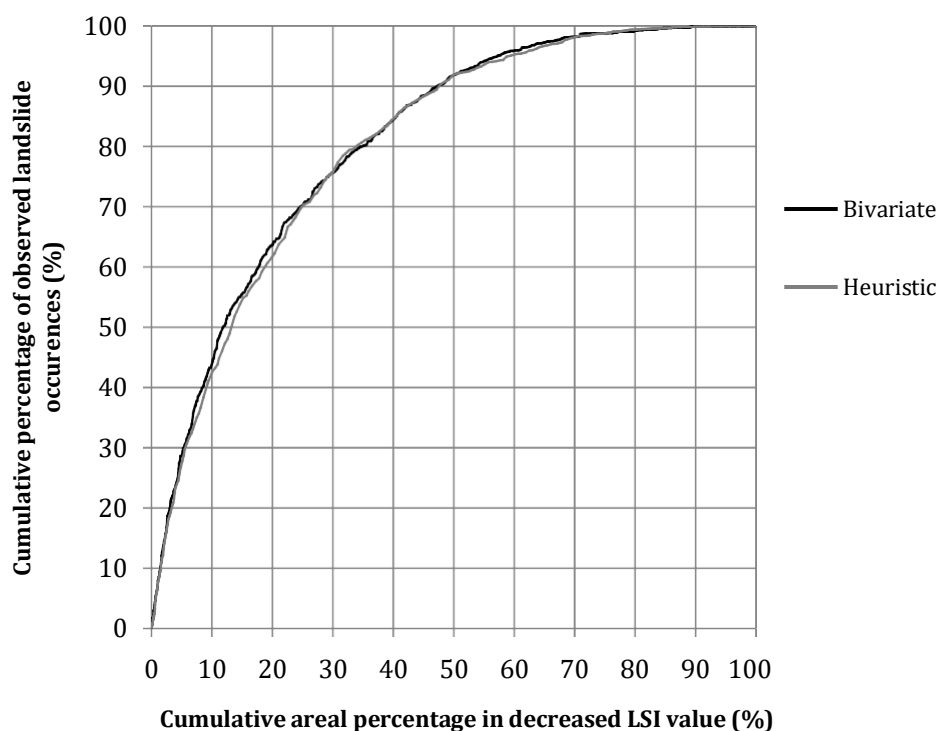


**Figure 5.10 Success rate curves of LSZ maps of heuristic and bivariate analysis methods**

It could be observed from the above graph that in both the maps 10% area of the high susceptibility zone contain about 40%, and 20% area contains 60% of the existing landslides. This also reflects the validity of the susceptibility maps in the existing slope instability conditions. The area under the curve for LSZ map of heuristic method is 80.78% and that of bivariate method is 81.29%. This means both the maps have ideal success rate of more than 80%.

### 5.4.3 Comparison Based on Agreed Area

The agreed area between LSZ maps of heuristic method and bivariate method expressed in pixels or km<sup>2</sup> or percentage of the total area is determined as the total area having the same landslide susceptibility in both LSZ maps. The result of the agreed area is displayed in [Table 5.7](#).

*Table 5.7 Agreed area and percentage area of heuristic and bivariate method, and area and percentage area of observed landslides in agreed area*

Susceptibility zones based on bivariate method	Susceptibility zones based on heuristic method	Area			Observed landslide area		
		(pixels)	(km <sup>2</sup> )	(%)	(pixels)	(km <sup>2</sup> )	(%)
Low	Low	<b>672032</b>	<b>67.22</b>	<b>47.57</b>	<b>1484</b>	<b>0.15</b>	<b>7.17</b>
	Moderate	38086	3.81	2.70	251	0.03	1.21
	High	8849	0.89	0.63	56	0.01	0.27
Moderate	Low	119533	11.96	8.46	1065	0.11	5.15
	Moderate	<b>149098</b>	<b>14.91</b>	<b>10.55</b>	<b>1969</b>	<b>0.20</b>	<b>9.52</b>
	High	29248	2.93	2.07	559	0.06	2.70
High	Low	4017	0.40	0.28	23	0.00	0.11
	Moderate	80164	8.02	5.67	1452	0.15	7.02
	High	<b>311806</b>	<b>31.19</b>	<b>22.07</b>	<b>13829</b>	<b>1.38</b>	<b>66.85</b>
<b>Agreed area</b>		<b>1132936</b>	<b>113.33</b>	<b>80.19</b>	<b>17282</b>	<b>1.73</b>	<b>83.54</b>
Total area		1412833	141.33	100.00	20688	2.07	100.00

The above table shows that the two susceptibility maps have 80.19% same content between them. The percentage of agreed landslide falling into agreed high susceptibility zone is 66.85%. It indicates that the predictive capability of both the maps is fairly good.

Even though heuristic method is subjective method where the researcher or an expert assigns weight and rating to the parameters based on personal judgement, the above results show that both the maps are nearly same with similar success rate and high agreed area. It can be concluded that both maps can be used in assessment of landslide hazards.

## **CHAPTER SIX**

### **CONCLUSIONS AND DISCUSSIONS**

Based on the present study focussed in the geological and landslide susceptibility mapping of the Ghurmi-Dhad Khola area, Eastern Nepal following conclusions and discussions are made.

#### **Conclusions**

The area is the southern part of the Okhaldhunga window and comprises of five lithological units, one of the Higher Himalaya and four of the Lesser Himalaya. The Lesser Himalayan Sequence is divided as the Para Khola Formation, Halesi Dolomite, Madhavpur Slates and Harkapur Formation. The Higher Himalayan Crystallines are described as a single unit.

The Para Khola Formation consists of red-purple quartzite, sandstone, red purple and green mottled shale with some bands of amphibolites. The Halesi Dolomite is seen only in a small area. It is probably carried from the east by the action of MCT. It consists of grey dolomite and is separated from the Higher Himalaya by the MCT and by another thrust from the Harkapur Formation. The Madhavpur Slates is predominantly slates with some calcareous beds. The youngest formation i.e. the Harkapur Formation is the mixed lithology of greenish-grey calcareous phyllite, slates, siliceous dolomite, light grey to pink quartzites and amphibolites. Its upper part is very deformed and fragile and the rocks are crushed.

The Higher Himalayan Crystallines comprises of psammitic schist, pelitic schist, banded gneiss, augen gneiss, infer-fingering granitic gneiss and few bands of white quartzite.

The MCT passes along the Sunkoshi River in the west, through the saddle of Hilepani in the central part and then along the Dudhkoshi River in the east.

There are 77 landslides in the area covering 2.069 km<sup>2</sup>. The landslides are observed in clusters with major clusters being in the Bhadare Khola, Bhalu Khola, Koltar and in Chuwabot.

Though not studied in detail about the morphology and the classification of the slides it could be said that a majority of the mass movement in the area are translational rock and soil slides.

Eight factors were considered for the landslide susceptibility analysis of the study area: geology, distance from fault-folds, distance from drainage, rock and soil type, land cover, slope aspect, slope angle and altitude.

The landslide susceptibility analysis was carried out by two different methods viz. index-based method of the heuristic approach and statistical-index method of the bivariate.

The landslide susceptibility zonation (LSZ) map prepared by the heuristic method showed 56.31% (79.583 km<sup>2</sup>) area in the low susceptibility zone whereas the area under medium and high susceptibility zones were 18.92% (26.743 km<sup>2</sup>) and 24.77% (35.001 km<sup>2</sup>) respectively. The high susceptibility zone consisted of 69.82% of total landslide with landslide density of 0.0413.

The LSZ map prepared by the bivariate method had 28.03% (39.611 km<sup>2</sup>) of area in high susceptibility, 21.08% (29.797 km<sup>2</sup>) in medium susceptibility and 50.89% (71.919 km<sup>2</sup>) area lies in the low susceptibility zone. The high susceptibility zone consisted of 73.98% of existing landslide with landslide density of 0.0386.

Both the maps had ideal success rate of more than 80% and had 80.18% mutual agreement with percentage of agreed landslide falling into agreed high susceptibility zone being 66.85%.

In both the maps Bhadare Khola (northeast Harkapur), Bhalu Khola, , north and south of Hilepani, Bahundada, Chuwabot, Phedigau and Majhigau lie in the high susceptible zone whereas villages like Sokhuditar, Ghurmi, Harkapur, Hilepani, Jortighat, Tallo Richwa, Mathillo Richuwa, Arubot, Unbhu, Udaypur, Manebhanjyang, Devithan, Sisneri are in less susceptibility zones. The distance form drainage, geology, slope angle and rock-soil type showed more effect on the stability of the slopes.



## **Discussions**

The landslide susceptibility analysis would have been more accurate had rainfall been considered as a causative factor. But due to the dearth of rainfall stations around the area, it was not considered. If true representative data of average rainfall of the area are to be found, the analysis would be more reliable.

The area should be studied in detail for more detailed soil-rock map. The rocks should be classified according to its strength. Similarly the soil should be classified according to their engineering properties. A detailed rock-soil map with rock strength and engineering properties of soil will be an added benefit in the susceptibility analysis.

During the infrastructure development works, care should be taken to avoid the high landslide susceptibility zones. Roads, buildings, irrigation canal etc. should be constructed in low hazard zones. In case of existing infrastructures that lie in the high susceptibility zone, slope stability works should be performed for the protection of the structures. For the Harkapur–Okhaldhunga road section passing through the high susceptibility zone in the Bhadare Khola and in north of Hilepani, slope stability measure should be carried out to protect the road from further deteriorating.

The landslide susceptibility map can be used to prepare the risk map and be used in the disaster management planning such as preparation of rescue routes, service centres and shelters.

## REFERENCES

- Acharya, G., De Smedt, F., Long, N.T., 2006. Assessing landslide hazard in GIS: a case study from Rasuwa, Nepal. *Bulletin of Engineering Geology and the Environment*, 65(1): 99-107 pp.
- Acharya, K.K., 2008. Qualitative kinematic investigations related to the extrusion of the Higher Himalayan Crystalline and equivalent tectonometamorphic wedges in the entral Nepal Himalaya. PhD thesis in geology. Universitat wien. Austria.
- Amatya, K. M., Jnawali, B. M., 1994. Geological map of Nepal. Department of Mines and Geology, ICIMOD.
- Arnold, M., Chen R.S., Deichmann, U., Dilley, M., Lerner-Lam, A.L., Pullen, R.E., Trohanis, Z., (eds), 2006. *Natural Disaster Hotspots, Case Studies*. The World Bank, Hazard Management Unit, Washington D.C., 184 pp.
- Cruden, D.M., Varnes, D.J., 1996. Landslide types and processes. In: Turner, A.K., and Schuster, R.L. (eds), *Landslides investigation and mitigation, special report 247*. Transportation Research Board, National Academy Press, Washington D.C. 36–75 pp.
- Dahal, R.K., Hasegawa, S., Nonomura, A., Yamanaka, M., Dhakal, S., Paudyal P., 2008. Predictive modelling of rainfall-induced landslide hazard in the Lesser Himalaya of Nepal based on weights-of-evidence. *Geomorphology*, 102: 496–510 pp.
- Dangol, V., Ulak, P.D., 2002. Landslide hazard mapping in Nepal: case studies from Lothar Khola (central Nepal) and Syangja district (western Nepal). *Journal of Nepal Geological Society*, 26: 99–108 pp.
- Deoja B., Dhital, M., Thapa, B., Wagner, A. (eds), 1991. *Mountain risk engineering handbook*. International Centre for Integrated Mountain Development (ICIMOD). Kathmandu. 875 pp.
- Dhakal, A.S., Amada, T, Aniya, M., 1999. Landslide hazard mapping and the application of GIS in the Kulekhani watershed Nepal. *Mountain Research and Development*, 19(1): 3-16 pp.
- Dhital M.R., 2005. Study of damage caused by rainfall in Hilepani-Jayaramghat-Diktel environment friendly road. Report submitted to the Rural Access Programme (RAP).

- Dhital, M.R., Shrestha, R., Ghimire, M., Shrestha, G.B., Tripathi, D., 2005. Hydrological hazard mapping in Rupandehi district, west Nepal. *Journal of Nepal Geological Society*, 31:59–66 pp.
- Dwivedi, S.K., Aryal, A. 1997. Geological map of area between the Sun Kosi River and the Kakaru Khola, Udaypur district, eastern Nepal. In: Dwivedi, S.K., 1997. *Geology of the area between the Sun Kosi River and the Kakaru Khola, Udaypur, eastern Nepal*. MSc Thesis in Geology. Tribhuvan University, Kathmandu. 49 pp.
- Gansser, A., 1964. *Geology of the Himalayas*. Interscience, London. 289 pp.
- Ghimire, M., 2001. Geo-hydrological hazard and risk zonation of Banganga watershed using GIS and remote sensing. *Journal of Nepal Geological Society*, 23: 99–110 pp.
- Guzzetti, F., Carrara, A., Cardinali, M., Reichenbach, P., 1999. Landslide hazard evaluation: a review of current techniques and their application in a multi-scale study, Central Italy. *Geomorphology*, 31(1-4): 181-216 pp.
- Hungr, O., Evans, S.G., Bovis, M.J., Hutchinson, J.N., 2001. A review of the classification of landslides of the flow type. *Environmental and Engineering Geoscience*, 7(3): 221-238 pp.
- Hashimoto, S. et al. (ed), 1973. *Geology of Nepal Himalayas*. Himalayan Committee of Hokkaido University. Sapparo. 292 pp.
- Hutchinson, J.N., 1988. General report: morphological and geotechnical parameters of landslides in relation to geology and hydrology. 5th International Symposium on Landslides, Balkema, Rotterdam, 1: 3-35 pp.
- Ishida, T., Ohta, Y., 1973. In: Hashimoto, S. et al. (ed), 1973. *Geology of Nepal Himalayas*. Himalayan Committee of Hokkaido University. Sapparo. 292 pp.
- Jackson, M., Bilham, R., 1994. Constraints on Himalayan deformation inferred from vertical velocity fields in Nepal and Tibet. In: Upreti, B.N., 1999. *An overview of the stratigraphy and tectonics of the Nepal Himalaya*. *Journal of Asian Earth Science*, 17: 577-606 pp.
- Johnson, R.B., DeGraff, J.V., 1988. *Principles of Engineering Geology*. 1st Ed., John Wiley and Sons, USA. 497 pp.
- Joshi, J., Majtan, S., Morita, K., Omura, H., 2000. Landslide hazard mapping in the Nallu Khola watershed, Central Nepal. *Journal of Nepal Geological Society*, 21: 21–28 pp.

- Kayastha, P., De Smedt, F., 2009. Regional slope instability zonation using GIS technique in Dhading, Central Nepal. In: Malet, J.P., Remaître, A., and Boggard, T. (eds), *Landslide Processes: From Geomorphologic Mapping to Dynamic Modelling*, CERG, France: 303-309 pp.
- Kayastha, P., Dhital, M.R., De Smedt, F., 2010. GIS based landslide susceptibility assessment in Nepal Himalaya: a comparison of heuristic and statistical bivariate analysis. In. Malet, J.P., Glade, T., and Casagli, N. (eds): *Mountain Risks: Bringing Science to Society*, CERG Editions: 121-128 pp.
- Koirala, M.P., Adhikary, P.C., 2007. Landslide hazard mapping in the Tinpile-Banchare Danda area, central Nepal. *Bulletin of Nepal Geological Society*, 24: 38-48 pp.
- Lee, K.I., White, W., Ingles, O.G., 1983. *Geotechnical Engineering*. 1st Ed., Pitman Books Limited, London. 504 pp.
- Lombard, A., Bordet, P., 1956. Une coupe géologique dans la région d'Okhaldunga (Népal Oriental). *Bulletin de la Société géologique de France*, Paris, vol. 6, sér. 6: 21-25 pp.
- Lombard, A., 1952. Les grandes lignes de la géologie du Népal Oriental. *Bulletin de la Société Belge de Géologie de Paléontologie et d'Hydrologie*, Bruxelles, vol. LXI, Fascicule 3: 260-264 pp.
- Lombard, A., 1953a. Présentation d'un profil géologique du mont Everest à la plaine du Gange (Népal Oriental). *Bulletin de la Société Belge de Géologie de Paléontologie et d'Hydrologie*, Bruxelles, vol. LXII, Fascicule 1: 123-129 pp. (with a cross-section).
- Lombard, A., 1953b. La tectonique du Népal Oriental. Un profil de l'Everest à la plaine du Gange. *Bulletin de la Société Géologique de France*, Série 6, vol. III: 321-327 pp (with a cross-section).
- Long, N.T., 2008. Landslide susceptibility mapping of the mountainous area in A Luoi District, Thua Thein Hue Province, Vietnam. PhD thesis in Engineering, Vrije Universiteit Brussel. 229 pp.
- Pandey, M.R., Tandukar, R.P., Avouac, J.P., Lavé, J., Massot, J.P., 1995. Interseismic strain accumulation on the Himalayan crustal ramp (Nepal). In: Upreti, B.N., 1999. An overview of the stratigraphy and tectonics of the Nepal Himalaya. *Journal of Asian Earth Science*, 17: 577-606 pp.
- Pantha, B.R., Yatabe, R., Bhandary, N.P., 2010. GIS-based highway maintenance prioritization model: an integrated approach for highway maintenance in Nepal mountains. *Journal of Transport Geography*, 18: 426-433 pp.

- Paudyal, P., Dhital, M.R., 2005. Landslide hazard and risk zonation of Thankot-Chalnakhel area, central Nepal. *Journal of Nepal Geological Society*, 31: 43–50 pp.
- Poudyal, C.P., Chang, C., Oh, H., Lee, S., 2010. Landslide susceptibility maps comparing frequency ratio and artificial neural networks: a case study from the Nepal Himalaya. *Environmental Earth Sciences*, 61: 1049–1064 pp.
- Ray, R.L., De Smedt, F., 2009. Slope stability analysis on a regional scale using GIS: a case study from Dhading, Nepal. *Environmental Geology*, 57: 1603-1611 pp.
- Safaei, M., Omar, H., Yousof, Z.B.M., Ghiasi, V., 2010. Applying geospatial technology to landslide susceptibility assessment. *Electronic Journal of Geotechnical Engineering*, Vol. 15, Bund. G, 677-696 pp.
- Sarkar, S., Kanungo, D.P., Kumar, P., Patra, A.K., 2008. GIS based spatial data analysis for landslide susceptibility mapping. *Journal of Mountain Science*, 5: 52-62 pp.
- Schelling, D. (1992) The tectonostratigraphy and structure of the Eastern Nepal Himalaya. *Tectonics*, 11: 925-943 pp.
- Seeber, L., Armbruster, J.G., 1981. Great detachment earthquakes along the Himalayan arc and long term forecasting. In: Upreti, B.N., 1999. An overview of the stratigraphy and tectonics of the Nepal Himalaya. *Journal of Asian Earth Science*, 17: 577-606 pp.
- Sharma, R.H., Shakya, N.M., 2008. Rain induced shallow landslide hazard assessment for ungauged catchments. *Hydrogeology Journal*, 16: 871–877 pp.
- Shrestha, S. B., Shrestha, J. N., Sharma S. R., 1984. Geological map of eastern Nepal. Department of Mines and Geology, Lainchaur, Kathmandu.
- Sikrikar, S.M., Rimal, L.N., Jäger, S., 1998. Landslide hazard mapping of Phewa lake catchment area, Pokhara, central west Nepal. *Journal of Nepal Geological Society*, 18: 335–341 pp.
- Stöcklin, J., 1980, Geology of Nepal and its regional frame. *Journal of the Geological Society of the London*, 137: 1-34 pp.
- Stöcklin, J., Bhattarai, K. D., 1977. Geology of the Kathmandu area and central Mahabharat range, Nepal Himalaya. Report of Department of Mines and Geology/ UNDP (unpublished), 86 pp.
- Terzaghi, K., 1950. Mechanism of landslides. In: Paige, S. (ed), *Application of geology to engineering practice*. New York, Geological Society of America (Berkey Volume): 83-123 pp.



- Thapa, P.B., Dhital, M.R., 2000. Landslide and debris flows of 19–21 July 1993 in the Agra Khola watershed of central Nepal. *Journal of Nepal Geological Society*, 21: 5–20 pp.
- Upreti, B.N., 1999. An overview of the stratigraphy and tectonics of the Nepal Himalaya. *Journal of Asian Earth Science*, 17: 577-606 pp.
- Upreti, B.N., Dhital, M.R., 1996. Landslide studies and management in Nepal. International Centre for Integrated Mountain Development (ICIMOD), Kathmandu. 87 pp.
- Van Westen, C.J., Rengers, N., Terlien, M.T.J., Soeters, R., 1997. Prediction of the occurrence of slope instability phenomena through GIS-based hazard zonation. *Geologische Rundschau*, 86(2): 404-414 pp.
- Van Westen, C., 1997. Statistical landslide hazard analysis. ILWIS 2.1 for Windows application guide. ITC Publication, Enschede: 73–84 pp.
- Varnes, D. J., 1958. Landslide types and processes, In: Eckel, E. B. (ed), *Landslides and engineering practice*. Washington D.C. Highway Research Board, Special Report 29, NAS-NRC Publication 544, 20-47 pp.
- Varnes, D.J., 1978. Slope movements, types and processes. In: Schuster, R.L., Krizek, R.J. (eds), *Landslide analysis and control*, National Academy Sciences, Washington D.C., 11-33 pp.
- Varnes, D.J., 1984. International Association of Engineering Geology Commission on Landslides and Other Mass Movements on Slopes: Landslide hazard zonation: a review of principles and practice, UNESCO, Paris. 63 pp.
- Varnes, D.J., 1996. Landslide Types and Processes. In: Turner, A.K., and R.L. Schuster (eds), *Landslides: Investigation and Mitigation*, Transportation Research Board Special Report 247, National Research Council, Washington, D.C. National Academy Press.
- Wagner, A., Leite, E., Oliver, R., 1988. Rock and debris slide risk mapping in Nepal, a user friendly PC system for risk mapping. In: Upreti, B.N., Dhital, M.R., 1996. *Landslide studies and management in Nepal*. International Centre for Integrated Mountain Development (ICIMOD), Kathmandu. 87 pp.